

From wind conditions to operational strategy: Optimal planning of wind turbine damage progression over its lifetime

Niklas Requate¹, Tobias Meyer¹, and René Hofmann²

¹Fraunhofer IWES, Bremerhaven, Germany

²TU Wien, Vienna, Austria

Correspondence: Niklas Requate (niklas.requate@iwes.fraunhofer.de)

Comment to reviewers

Due to the restructuring of the paper, highlighting the differences could not be done for the complete document as a whole. Therefore, we highlighted differences for each section separately. For each section, we comment how this section relates to the previous document if there was a change. The new structure is also described in the response to the reviewers.

Abstract. Renewable energies have an entirely different cost structure than fossil fuel-based electricity generation. This is mainly due to the operation at zero marginal cost, whereas for fossil fuel plants, the fuel itself is a major driver of the entire cost of energy. For a wind turbine, most of the materials and resources are spent up front. Over its lifetime, this initial capital and material investment is converted into usable energy. Therefore, it is desirable to gain the maximum benefit from the utilized materials for each individual turbine over its entire operating lifetime. Material usage is closely linked to individual damage progression of various turbine components and their respective failure modes.

Within this work, we present a novel approach for an optimal long-term planning of the operation of wind energy systems over their entire lifetime. It is based on a process for setting up a mathematical optimization problem that optimally distributes the available damage budget of a given failure mode over the entire lifetime. The complete process ranges from an adaptation of real-time wind turbine control to the evaluation of long-term goals and requirements. During this process, relevant deterministic external conditions and real-time controller setpoints influence the damage progression with equal importance. Finally, the selection of optimal planning strategies is based on an economic evaluation. The method is applied to an example for demonstration. It shows the high potential of the approach for an effective damage reduction on different use cases. The focus of the example is to effectively reduce power of a turbine under conditions where high loads are induced from wake-induced turbulence of neighbouring turbines. Through the optimization approach, the damage budget can be saved or spent under conditions where it pays off most in the long-term perspective. This way, it is possible to gain more energy from a given system and thus to reduce cost and ecological impact by a better usage of materials.

1 Introduction

20 Meeting the rising demand for energy without using fossil fuels is probably one of the greatest challenges of our time. Wind energy plays a key role in achieving this worldwide, and the wind industry has been developing to a mature and effective branch of technology. Nevertheless, energy production will always involve the use of materials and resources. For a wind turbine, this includes the production of large complex components like the tower, the rotor blades and the generator, but also the use of land on- and offshore as well as continuous operating costs due to maintenance and repair activities.

25 Therefore, it is desired to gain the maximum benefit from the utilized materials for each individual turbine over its entire ~~operating lifetime. The materials~~ lifetime. Materials will be used up through the operation in many different ways. The usage is closely linked to individual failure modes of various turbine components. While some of these failure modes need to be avoided through advancements in design and robustness to environmental conditions, other failure modes are highly influenced through the operational strategy. Especially fatigue damage is strongly influenced by induced loads which depend on the external
30 conditions in combination with the operational control of the turbine. Even with the smartest individual control solutions for load reduction like e.g. individual pitch control and active damping, there will always be some trade-off between power production and induced damage which cannot be fully prevented. Additionally, load reducing effects for some failure modes might have negative effects on others.

With the ~~experience and~~ development of a maturing wind industry, standard procedures for the design of wind turbines have
35 been established for finding a reasonable trade-off between induced damage and power production. This way, wind turbines be operated for at least 20 years under various conditions from the environment and the grid. While the external conditions of each turbine are highly individual, wind turbine design can only consider site-specific conditions to some extent, e.g. by type certificates for different wind classes IEC (2019). In order to operate each turbine at its individual optimal balance of induced damage and power production, an adaptive operation based on information of the current condition and performance
40 is required. A concept for such an operation is proposed through reliability(-adaptive) control which can principally be applied to any system where components are used up from operation, i.e. are subject to degradation. The reliability controller is implemented as a closed-loop supervisory controller which adapts the system such that it meets predetermined reliability objectives. Within this concept, it is important to distinguish between the real-time controller directly interacting with the actuators of a system and the outer supervisory control. The outer loop runs on a slower time scale and can send setpoints to
45 the real-time controller.

Within this work, a method for finding an optimal long-term operational planning which already includes the available setpoints for the wind turbine real-time controller is presented. Thus, it contributes to the development of a reliability(-adaptive) control loop for wind turbines by creating a desired operation which is necessary for a closed-loop operation. It also brings advantages in itself for an open-loop operation. ~~Within this chapter, the method is first embedded into the context
50 of reliability(-adaptive) control (Sect. 1.1). Afterwards, the objectives of this work are further elaborated in Sect. 1.2 and the methodology for creating an optimal planning is explained in Sect. 1.3.~~

1.1 State of the art

A concept for a Safety and Reliability Control Engineering (SRCE) including a supervisory reliability controller, which uses information about the current state-of-health, was introduced in Söffker and Rakowsky (1997) and further discussed e.g. in 55 Rakowsky (2005) and Rakowsky (2006). In Meyer (2016) a reliability controller based on the health index, used as a measure for the state-of-health, for a mechatronic system was implemented and validated. On the one hand, the application of such an approach for wind energy systems has a high potential due to the highly individual site and turbine specific operating and environmental conditions as well as ageing characteristics of various components (Meyer et al., 2017). On the other hand, the complexity of the coupled system, the interaction of wind turbines in a wind farm as well as constraints from operating 60 and maintenance strategies, market conditions, grid requirement and nevertheless certification processes lead to a challenging interaction of different areas. One of the major aspects for the operation of a reliability controller in a closed-loop is the information about the state-of-health of the considered system. While wind turbines are equipped with various sensors and associated condition monitoring systems (CMS) or structural health monitoring (SHM) systems, the prognosis of the actual state-of-health and the associated remaining useful lifetime (RUL) still requires a lot of research and development. In Beganovic 65 and Söffker (2016), an overview of signal-based monitoring methods with a focus on the usage for online fault detection and advanced control is provided. In Do and Söffker (2021), an overview of management and control strategies for wind turbines based on health prognostics is provided. Both papers clearly state that further investigation is needed to determine the state-of-health. Additionally, the high requirements for an adaptive controller due to the multi-objective nature of the problem under various loading condition is also mentioned. Nevertheless, the full advantage of health monitoring combined with advanced 70 reliability control strategies can only be fully exploited with further development in each of the fields, which can later be combined to an integrated approach.

There are two major advantages which result from the use of closed-loop structure for controlling the reliability. On the one hand, it enables a synchronization with maintenance strategies or planned decommissioning. On the other hand, it allows extending the lifetime of a system by switching to a load reducing control configuration at any point in time. The latter point 75 is specifically addressed in the concept of life extending control, where a concept was introduced in Lorenzo and Merrill (1991). This concept is more oriented towards fatigue damage and thus also well applicable for wind turbines. The approach was pursued for wind turbine operation in Santos (2006) and the associated patent (Santos, 2008). In the study, the wind turbine actuators are directly modified by a model predictive control algorithm, which receives setpoints for the degradation of the turbine from a supervisory control loop. Comparable concepts based on an online fatigue accumulation using online 80 rainflow counting were also followed by Loew et al. (2020) and Njiri et al. (2019). The latter is clearly related to the concept of reliability adaptive control, which was explained above. In all three of the applications, the controllers are tested on rather short timeframes of at maximum 600 seconds so that long-term benefits from the methods can not yet be fully considered. Long-term effects of adapting control strategies during operation for lifetime extension are examined in Pettas et al. (2018) and Pettas and Cheng (2018). In Requate and Meyer (2020), the concept of reliability control is implemented by switching between 85 different down- and uprating configurations to follow a predetermined desired degradation for several years. Dependent on the

desired target, a lifetime extension by several years can be reached. While the concept of directly adapting the turbine actuators according to the desired planning targets might have a higher theoretical potential because its reaction is more flexible, the concept of switching between different configurations seems to be more straightforward to implement for existing structures for wind turbine and wind farm control concepts. It also facilitates a guarantee for a safeguarded operation in all of the selected configurations. The combination of both concepts might offer additional advantages in the future.

In all of the mentioned work, the aspect of planning the operation up until the end of a wind turbine's lifetime has not yet been addressed in much detail. This becomes even more relevant in the context of wind farm control where the higher level constraints like the market prices, maintenance strategies, planning of decommissioning are relevant. ~~Wind farm control~~
In Kölle et al. (2022a), the results of several participants on showcases for wind farm flow control under consideration of electricity prices are discussed. The influence of operation on loads and damage is only considered by one of the five participants for a single turbine. In general, wind farm control has gained growing interest of research and also industry in recent years. One major focus of research was the mitigation of wake effects, which decrease power production but increase loads on downstream turbines (Dimitrov, 2019). Wake steering by yaw, but also derating¹ of the upstream turbines can be used, to increase the overall power production of a wind farm. In addition to increasing the power production, the influence on the loads and lifetime of the wind turbines of such methods are also examined (Andersson et al., 2021; Nash et al., 2021; Meyers et al., 2022; Houck, 2022). At first, the focus is not to increase the loads above the limits of certification, but the use of wind farm control for active load reduction is also examined in several studies (Bossanyi, 2018; Kanev et al., 2018, 2020; Harrison et al., 2020). Concepts for an integrated control of wind farms covering the complete range from short-term demands for grid services up to long-term objectives for reliability are required (Eguinoa et al., 2021; Kölle et al., 2022b). Therefore, combining the approaches of wind farm control with reliability adaptive control offers a high potential for a truly optimal operation, e.g. by intelligently managing which turbines should take over grid services in certain situations based on their current state-of-health and a planning until the end of the desired lifetime. For future energy systems, the interconnection to storage systems or power-to-X technologies and their reliability and degradation mechanisms also need to be considered.

Since the future damage progression of a system depends on the way it is operated, it is important to integrate the adaptive control behaviour into the planning process. Implicitly, this is done when sector management is applied to avoid high loads from an upstream turbine. Previous studies have shown, that it is possible to balance energy and loads with sector management strategies using derating (Bossanyi and Jorge, 2016).

A method for derating a wind turbine is integrated into any modern wind turbine to comply with grid requirements in one way or the other. Additionally, it can be used as an instrument to either reduce the effects from wake on the downstream turbine or to reduce loads of the turbine itself. The derating of the turbine is a setpoint to the wind turbine's real-time controller. The implementation of the derating method by parameters within the real-time controller thus depends on the objective and also on the individual dynamic behaviour of each turbine (Meyers et al., 2022; Houck, 2022). Even reducing damage from heavy rain

¹In general, there are various terms for reducing the power of a wind turbine and the usage often depends on the context. In wind farm control, the term axial-induction control is often used. Also down-regulation or curtailment are prominent terms. The latter is often referred to in the context of requests by the grid operator. The term derating is used throughout this work.

on the leading edge of the blades might be a possible objective for rotor speed reduction, besides the more common fatigue damage (Bech et al., 2018). ~~Other studies that are more focused on the specific objectives of this paper are presented at the appropriate part in the text, mainly in Sect. 2. The objectives are defined in the next section.~~

1.2 Objectives

Comment to reviewers

In this section, the list of bullet points was replaced with Figure 1. Less details are given to each step here. The details are moved to the separate sections for each step.

~~Overall, we have identified three major requirements to allow for a reliability-adaptive closed-loop operation. At first, methods for load reduction which reduce performance or conflict with other objectives need to be available within the wind turbine real-time controller. This requirement is definitely fulfilled for real-time controller wind turbines and wind energy systems, e.g. by using derating. The main difficulty lies in determining the amount of damage reduction for the individual failure modes of a turbine under various external input conditions. This is directly connected to the second requirement: The closed-loop controller needs continuous feed-back on the performance of the turbine, ideally on the state-of-health for each failure mode. This involves further research and development on condition and health monitoring, which is an ongoing process as discussed in Sect. 1.1. The third requirement consists of a planned desired operation of the system up until the desired lifetime, which is addressed within this work.~~

We assume a basic setup for a supervisory reliability control loop of a wind turbine or a complete wind farm by separating into different stages acting on different time scales. On the real-time stage, the dynamic loads of a wind turbine result from the interaction between the real-time wind turbine controller and the external conditions from the environment and the grid. Those loads slowly induce damage to the wind turbine. The supervisory reliability control loop acts on a time ~~scale~~ scope of 10 minutes up to several days because such a time ~~scale~~ scope allows for an appropriate performance evaluation of the wind turbine in terms of damage progression and power production. On this operating stage, setpoints are sent to the real-time controller of the wind turbine. The planned desired operation determines the targets for this stage which result from the long-term reliability objectives, i.e. the planned damage progression. Because of the dependency between reliability and operation, the desired operation already needs to consider the influence of adaptive control on the damage while at the same time focusing on long-term planning decisions and economic benefits. An overview of a wind farm which is operated using adaptive operation on these two stages is given in Fig. 1. The long-term planning (Planning stage on left-hand side of the figure) can either be used in an open-loop by providing setpoints to the wind turbine controller for specific input conditions or a target damage progression of the reliability control loop. In both cases, it should cover most relevant deterministic effects on long-term damage progression in an optimal way. Through a closed-loop behaviour on the operating stage, it is additionally possible to react to the actual performance of the wind turbine, including the current state-of-health and additional current inputs from weather or market price conditions (Right-hand side of the figure). At the same time, the long-term objectives are still met. A re-adaptation of the planning required when large deviations of the original planning occur or if the long-term

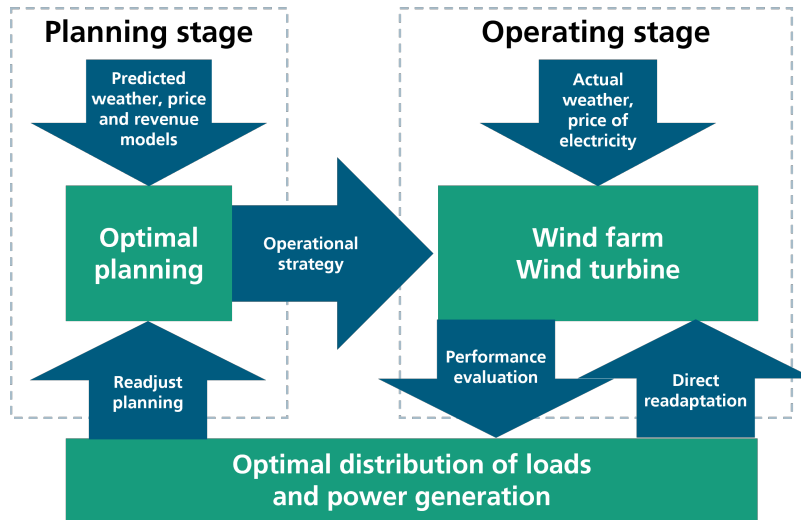


Figure 1. Overview of adaptive wind farm operation separated in to planning and operating stage

Comment on figure

Color of figure 1 is updated. "Adapt wind farm operation" is replaced with "Operational strategy" on the error in the centre.

objectives change. Thus, it is not a real closed loop operation, but it can also be applied when open-loop setpoints are sent to the real-time controller. It should just be applied after longer time periods of months or several years.

The long-term objectives for wind turbine operation are specifically driven by fatigue damage progression, which is an important failure mode for wind turbine principal components like the tower and the blades. For an optimal material usage, fatigue budget is ideally fully used up at the desired lifetime while a maximum amount of energy has been produced during this time. Thus, balancing the trade-off between induced damage and power production over the whole range of external conditions and under consideration of their frequency of occurrence is required. The goal is to find a planning method, which distributes the fatigue damage optimally over the planned operating time by saving the fatigue budget where it pays off most, i.e. where loads are high, but energy production is low. This is possible because of the nonlinear relationship between external conditions, load reducing control features and induced damage. When a turbine is subjected to high wake induced turbulence, for example, the relationship between induced damage and produced energy is definitely worse than for a turbine operating at the same wind speed at a low turbulence. The key question for an optimally planned target distribution is to decide by how much the damage should be reduced through adaptive control so that the long-term objectives are met. To answer this question, a method to find an optimal planning through mathematical optimization for an individual wind turbine is built up.

1.3 Methodology

In order to create a planning method which fulfills the objectives, the complete process from an adaptation of real-time wind turbine control to the evaluation of long-term goals and requirements needs to be covered. During this process, the influence on damage progression of relevant deterministic external conditions is just as important as that of real-time controller setpoints.

The key part of our proposed method consists of the formulation of a mathematical optimization problem, where the aim is to meet long-term objectives, such as maximum power or revenue over the entire lifetime, by finding an individual trade-off between induced damage and power production for each relevant operational condition.

For application of our method to a given system, it is crucial to know how it interacts with its environment. For this, the system boundary must be well-defined beforehand. It forms the basis for definition of environmental inputs, for setpoints of the real-time controller, as well as for the damage of different failure modes and performance measures such as energy production.

We identified a four-step process to create the optimal planning for this well-defined system within its boundaries, cf. in Fig.2.

Step 1: Provide adaptable real-time controller of the wind turbine

The setpoints of the real-time controller of the system directly influence the trade-off between induced damage and energy production. To make use of this, several sets of setpoints need to be provided such that different trade-offs can be selected accordingly.

Step 2: Build surrogate models for damage progression and energy production

In order to optimally distribute the fatigue budget over the system's lifetime, it must be possible to evaluate the effect of changes in the optimization variables with little computational cost. This necessitates the use of surrogate models, which represent the relationship between external conditions and setpoints of the controller to damage and energy. Thus once the real-time controller is finalized, such surrogate models need to be setup.

Step 3: Determine optimal condition-based operational strategies for lifetime planning

By combining the surrogate models with a statistical frequency distribution of the relevant external conditions defined by the

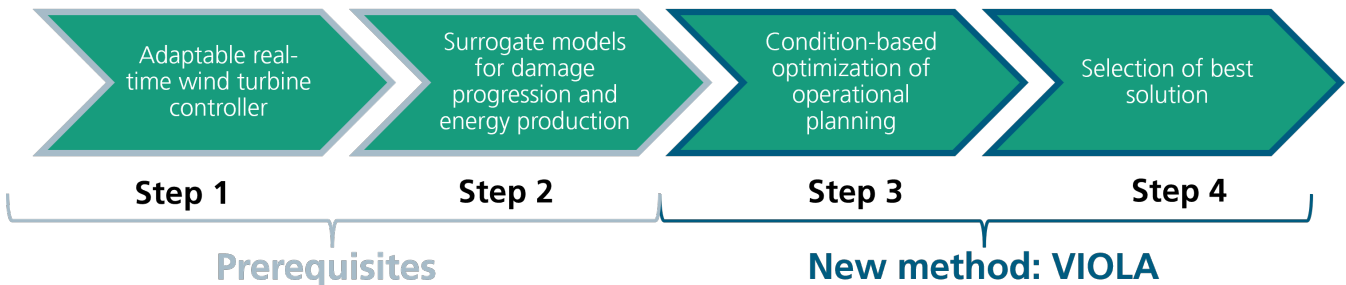


Figure 2. Four step process for optimal planning, subdivided into prerequisites and new method

system boundaries, a rough long-term prediction of the damage progression can be obtained. This model of damage progression forms the basis of an optimization problem, in which the objective is to optimally distribute the available damage budget over the entire operating time. The optimization variables, i.e., the means to influence system operation, are the real-time controller setpoints for all external conditions. They are optimized for all external conditions at once. This way, performance is maximized while the total damage budget is optimally distributed.

Step 4: Select economically best operational lifetime planning strategy

The optimization from step 3 yields multiple results, where each one represents an individual trade-off between energy production and damage. The selection of a single optimal planning becomes possible, by evaluating economic aspects of the results from step 3.

The four steps not only allow for a feasible computation time, but they also lead to an easily explainable result after each step, which is in stark contrast to more integrated approaches. The four steps can principally be applied to any system which is subject to a strong coupling of control setpoints and external conditions. Due to the high influence of wind conditions on the fatigue damage of wind turbines, wind energy systems represent a prime example for its application. Within this work, we concentrate on fatigue damage because it is the most significant failure mode for long-term operation of wind turbines (as already mentioned in Sect. 1.2).

For optimizing the distribution of the fatigue budget over the system's lifetime, it must be possible to evaluate the effect of changes in the setpoints of the adaptable real-time controllers with low computational effort. The setpoints of the real-time controller of the system directly influence the trade-off between induced damage and energy production. Once the adaptable real-time controller is provided, surrogate models, can be set up. They represent the relationship between external conditions and setpoints of the controller to damage and energy. These first two steps 1 and 2 are necessary but existing prerequisites for the long-term optimization of the operation. They need a careful selection and have a strong influence on the quality and the validity of the results. The optimal operational planning is found by steps 3 and 4 of the process. Both of the steps are part of the proposed long-term planning method which we name VIOLA (Value Integrated Optimization of Lifetime Asset operation). The optimization problem is built up in step 3. This step still yields multiple results, where each one represents an individual trade-off between energy production and damage. The selection of a single optimal planning becomes possible, by evaluating economic aspects of the results from step 3.

The four steps not only allow for a feasible computation time, but they also lead to an easily explainable result after each step, which is in stark high contrast to more integrated approaches. The four steps can principally be applied to any system which is subject to a strong coupling of control setpoints and external conditions. Due to the high influence of wind conditions on the fatigue damage of wind turbines, wind energy systems represent a prime example for its application. Within this work, we concentrate on fatigue damage because it is the most significant failure mode for long-term operation of wind turbines (as already mentioned in Sect. 1.2).

1.4 Outline of the remaining paper

220 The ~~above-mentioned~~above-mentioned four-step process ~~form-forms~~ the core of the remaining paper. At first, ~~their~~the theoretical background and a more in-depth ~~explanation~~explanation for the approach are given in Sect. 2. ~~Afterwards, the process is applied to~~The process is demonstrated with an application example, ~~a small wind farm with 9 generic 7.5 MW wind turbines.~~ The focus of the example is to effectively reduce power of a considered turbine under conditions where high loads are induced from wake-induced turbulence of ~~a neighbouring turbine. The system is introduced and its boundaries are defined in Sect.~~
225 ~~3.1. neighboring turbines.~~ In Sect. 3, the considered system is defined. Also, ~~its prerequisites are introduced and implemented, resulting in surrogate models usable for the optimization.~~ Afterwards, the ~~steps are long-term optimization process VIOLA is presented and~~ applied to the example in Sect. ~~??.~~The applied process and the results are discussed in Sect. ~~??~~5 before the findings are concluded, and an outlook is given in Sect. 6.

2 ~~Theoretical background~~to application of four-step planning procedure

Comment to reviewers

The theoretical background only contains the former introduction to the chapter and subsection 2.1. Subsection 2.1 is split up into Section 2.1 and 2.2. The content of former sections 2.2 to 2.5 has been shortened and moved to other sections.

230

The basic idea of our method is to optimally distribute the induced damage over the operating time. With this, we assume a continuous and deterministic increase in damage over time, as depicted in Fig. 3.

Damage always refers to damage which directly and exclusively contributes to a certain failure mode fm . The lifetime of a system or a component is reached when the damage for a failure mode D_{fm} reaches the value 1, which is equivalent to 100%
235 of the available damage budget. Using a reference operational strategy \bar{u}^{ref} , the value ² $D_{fm}(\tau^{ref}; \bar{u}^{ref}, \cdot)^2$ is reached at the reference lifetime τ^{ref} . Our goal is to use a modified operational strategy \bar{u}^{opt} over a freely chosen operation period τ^{life} to distribute the damage $D_{fm}(\tau^{life}; \bar{u}^{opt}, \cdot)$ in such a way that maximum energy yield or largest economic profit is obtained. Fig. 3 also depicts a time ~~increment span~~ $\Delta\tau$, which for wind energy problems is commonly selected as one calendar year because it captures the seasonal variations of the wind. Thus, the damage over this time span is referred to as annual damage $\Delta D_{fm}(\bar{u}, \cdot)$
240 for any operating strategy \bar{u} . Within the time ~~increment span~~ $\Delta\tau$, the damage ~~rate increment on the minutes scope~~ is not constant. Instead, it changes over time due to ~~e.g., seasonal~~the variation of environmental conditions, and correspondingly

²~~Note that in our notation which we distinguish between variables, i.e., values that can be changed, and parameters, which are fixed. They are separated by a semicolon. If additional variables or parameters exist but are not important for a certain passage, we omit them to improve readability and replace them with a central dot --.~~

²Note that in our notation we distinguish between inputs and parameters of the defined function. Parameters are assumed to be fixed for a specific use case. They are separated by a semicolon, where the function inputs are in front of the semicolon. If additional parameters exist but are not important for a certain passage, we omit them to improve readability and replace them with a central dot (\cdot). So for $D_{fm}(\tau^{ref}; \bar{u}^{ref}, \cdot)$, τ^{ref} is an input, \bar{u}^{ref} is a set of parameters and \cdot denotes that additional parameters are omitted.

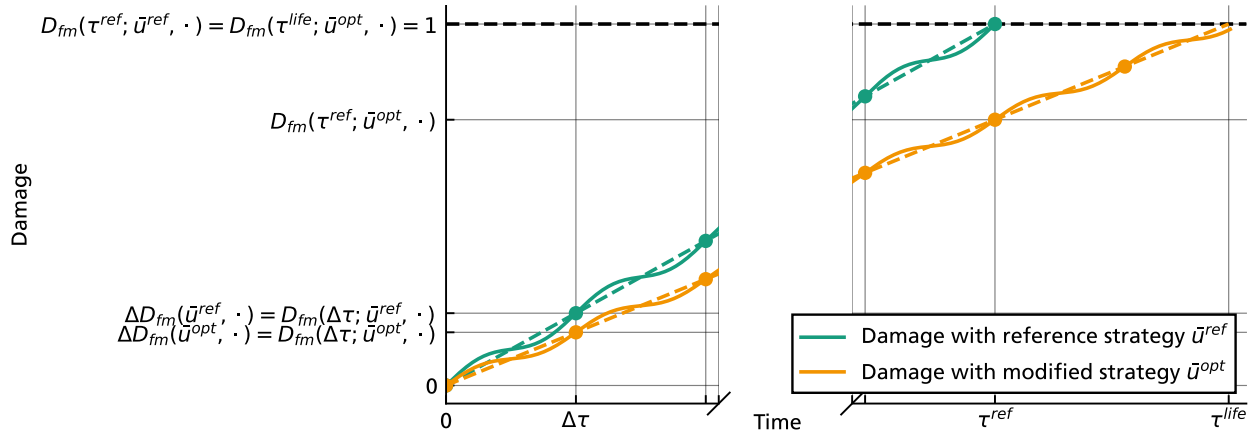


Figure 3. Illustration of damage progression over time for a reference (green) and a modified-an optimized operational strategy (yellow). Solid lines: Representation of continuous damage progression at a time scope of minutes. Dashed lines: Linear approximation of damage progression at a time scope of $\Delta\tau \approx 1\text{year}$.

varying control setpoints. The continuous damage progression at the more detailed time-scale-minutes scope is indicated in Fig. 3 by the wave-like behaviour of the increasing damage value (solid curves). This relationship from environmental input conditions and setpoints to damage rate-increment is highly nonlinear in both dimensions, which makes it possible to compensate for high-damage environmental conditions by using low-damage setpoints. For now, the effect of seasonal variation on damage and energy yield is fully included in the final value after one-time-increment-the time span $\Delta\tau$. We use this as the basis of our optimization.

It is immediately apparent that for given values at discrete time increments $\Delta\tau$ only, there is a linear relationship between the total damage $D_{fm}(\tau; \bar{u}, \cdot)$ and time $\tau = Y \cdot \Delta\tau$ exists τ for any operational strategy \bar{u} . But this holds for given values at discrete time points $\Delta\tau$ only, i.e. for $\tau = Y \cdot \Delta\tau$. The value Y is the number of time increments-spans to the full time period τ , e.g. i.e., the number of operating years when $\Delta\tau$ represents one year with the annual damage being the slope of the linear function. This is expressed by

$$D_{fm}(\tau; \bar{u}, \cdot) = D_{fm}(\Delta\tau; \bar{u}, \cdot) \cdot Y = \Delta D_{fm}(\bar{u}, \cdot) \cdot \tau. \quad (1)$$

where $\Delta D_{fm}(\bar{u}, \cdot)$ is the damage increment over one time increment $\Delta\tau$.

We now assume that using an optimal operating strategy \bar{u}_{opt}^{opt} , we achieve an optimized lifetime τ^{life} . During this changed lifetime, the entire damage budget is spent, i.e., $D_{fm}(\tau^{life}; \bar{u}_{opt}^{opt}, \cdot) = 1$. The modified lifetime period using \bar{u}_{opt}^{opt} is then simply given by inserting the optimized values in Eq. (1) and resolving for τ^{life} :

$$\tau^{life} = \frac{D_{fm}(\tau^{life}; \bar{u}_{opt}^{opt}, \cdot)}{\Delta D_{fm}(\bar{u}_{opt}^{opt}, \cdot)} = \frac{1}{\Delta D_{fm}(\bar{u}_{opt}^{opt}, \cdot)}. \quad (2)$$

Thus, our aim is now to find a strategy \bar{u}^{opt} which optimally changes the ~~damage-increment~~ annual damage to $\Delta D_{fm}(\bar{u}^{opt}, \cdot)$
260 ~~within the fixed period $\Delta\tau$. The damage-increment generally depends on environmental conditions, e.g., incoming wind conditions, and setpoints of any applied strategy \bar{u} .~~

Computing the modified lifetime with Eq. (2) can result in *any* timespan τ^{life} . However, due to seasonality and the associated nonlinearity ~~, which is depicted as solid curve in Fig. 3, within~~ the time ~~increment-span~~ $\Delta\tau$, Eq. (1) only holds true for $Y \in \mathbb{N}$. This ~~usually~~ applies for τ^{ref} , but the resulting value ~~for~~ τ^{life} from Eq. (2) depends on the optimized damage increment
265 $\Delta D_{fm}(\bar{u}^{opt}, \cdot)$, ~~which-and~~ can take up any value, ~~and~~. It is in turn not restricted to natural numbers. ~~However, for a longer timespan τ^{life}~~ For a long timespan τ^{life} , the resulting error is small ~~compared to the~~ in comparison to uncertainties resulting from the ~~overall extrapolation process, and can be neglected when the modified lifetime is computed~~ assumptions for the deterministic long-term fatigue modelling approach.

That the assumption

$$270 \quad \tau^{ref} = Y \cdot \Delta\tau, Y \in \mathbb{N}. \quad (3)$$

holds is due to a suitable scaling of $\Delta D_{fm}(\bar{u}^{ref}, \cdot)$. Among other things, this includes the assumptions that the damage budget is completely used up under the reference strategy \bar{u}^{ref} and that the damage increment is always the same for each time increment $\Delta\tau$. The latter is based on the standard approach in the design process of wind turbines, where the damage ~~progress during one year-increment of a short time interval Δt (10 min to 1 hour)~~ is extrapolated to ~~periods longer than 20 years. This is realized~~
275 ~~by using frequency distributions~~ the annual damage progression using a frequency distribution of the input conditions.

~~With the basic steps having been defined in Sect. 1.3 and a formally sound mathematical basis of our approach, we can now go into more details of further prerequisites,~~ i.e. to the time periods $\Delta\tau$ and τ^{life} respectively. Therefore, the damage increment $d_{fm}(x, u)$ under the external input conditions $x \in X$ and the control setpoints $u \in U$ needs to be known. Here, X defines the space of selected input conditions for the specified system boundaries and U is the space of possible control
280 ~~setpoints. In principle, $d_{fm}(x, u)$ can be obtained from an arbitrary method for a specific failure mode. Within this work, we use the standard approach for wind turbine fatigue modelling based on the assumption of a linear damage accumulation by Palmgren and Miner (Miner, 1945; Sutherland, 1999).~~

For the long-term calculation of damage and fatigue, different time scopes are relevant. Fig. 4 shows an overview of the different time scopes in interaction with the surrogate models. It also gives an overview of terms and symbols used. For the surrogate models, inputs and outputs on the minute scope are decisive. This relation is generated by using high-fidelity simulations on the second seconds and their evaluation. At the seconds scope, the control setpoints u are transferred into the individual steps ~~real-time controller of the wind turbine. Multiple of such simulations are carried out to create the surrogate models. Thus, the creation of the models finalizes the required prerequisites of steps 1 and 2 according to Fig. 2. The optimization process is later carried out on the annual scope, where the surrogates are evaluated to calculate the annual~~
285 ~~damage and the annual energy depending on different operational strategies. Finally, the annual values can be used, to compute the lifetime total energy and total damage. Before those can be used for the long-term optimization process in steps 3 and~~
290 ~~the lifetime total energy and total damage. Before those can be used for the long-term optimization process in steps 3 and~~

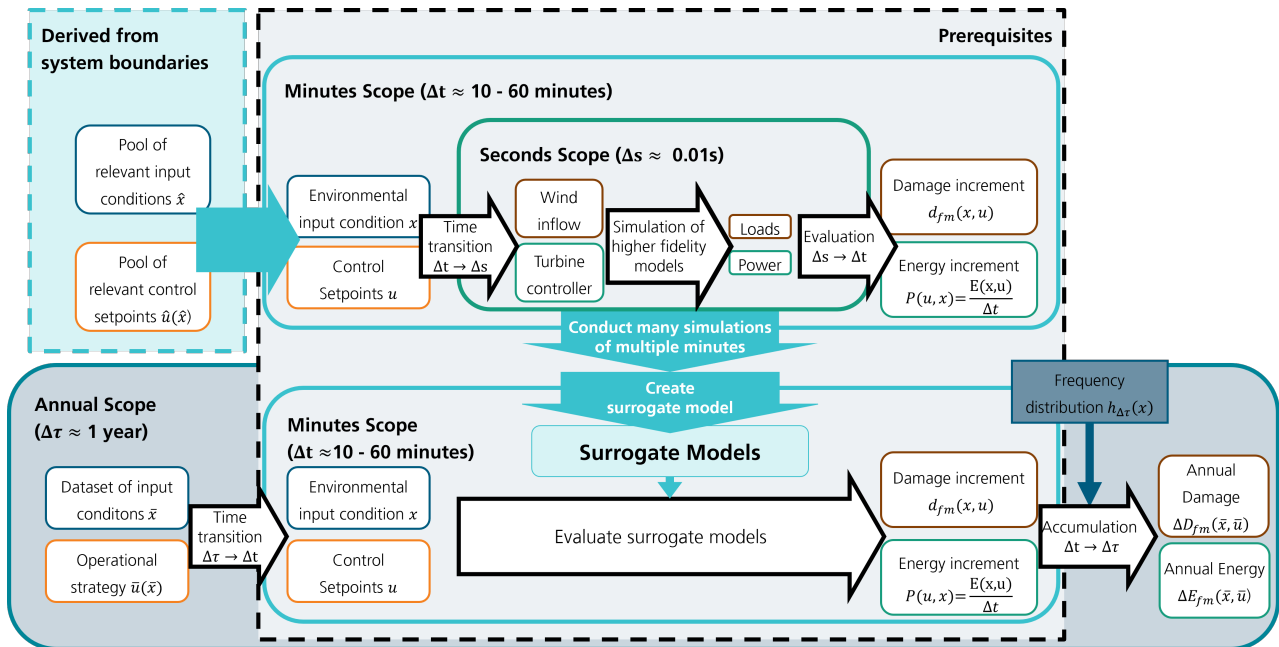


Figure 4. Overview of time scopes for creation and usage of surrogate models. The white rectangles with rounded curves denote in- and outputs on different time scopes. The white arrows describe a transition from input to output with a corresponding model. The rectangle in the center contains the prerequisites and ends with the creation of surrogate models which can be evaluated on the minutes scope. The creation process is depicted by the bright blue arrows, starting from the pool of input samples. Within the annual scope, the surrogate models are used to compute the annual value with the frequency distribution as an additional input.

Comment on figure

Figure 4 is entirely new. It has been added to clarify the different time scopes and the full process for creation and usage of surrogate models.

4, we explain the relationship between the different time scopes with respect to loads, fatigue damage, lifetime, and energy production on a theoretical level.

2.1 Long-term fatigue damage progression and energy production depending on external conditions and operational planning

295

The standard approach in wind turbine design is the extrapolation of wind turbine loads from simulations to the design lifetime of e.g., 20 or 25 years. It is also a requirement for the certification of a turbine, defined in standards like (IEC, 2019; DNV GL, 2016). In the standards, design load cases (DLCs) determine the external conditions. To cover a wide range of sites, reference classes of wind conditions are defined, and conservative assumptions are often made. Currently, a fixed operational strategy

300 is assumed for each turbine. ~~Therefore, there is currently no standardized process for the certification of wind farm control, e.g., by wake steering, since a subsequent adaptive adjustment of the turbine control is not covered by turbine certification standards. Integrating wind farm flow control into current and future certification procedures is part of ongoing work and discussions (Kölle et al., 2022b). In the case of general adjustments to the operational strategy, such as through adjustments to the power curve or a power boost, evidence must be provided that the design damage budget is not exceeded.~~ The major
 305 difference between standard design calculations for fatigue damage and the presented approach for optimal planning is the explicit integration of the control setpoints as a dependent variable on the external conditions, which can adaptively be selected and thus used as an optimization variable.

To cover the dependency of control on the external conditions, we assume that for each external input condition $x \in X$, there are one or multiple setpoints for the real-time controller $u(x) \in U$ that can be selected. ~~The sets X and U will later on be clearly defined based on the system boundaries. The external input conditions are defined over a~~ Both are defined on the
 310 minutes scope and thus valid over the time increment Δt , ~~and subsequently all of the dependent quantities are as well. It is at the time scale of the supervisory control loop, i.e., between minutes and hours. The idea now is to bin each operating condition separately, and then to~~ To determine the relative frequency for each combination of input conditions, a binning is required. Each combination of conditions is allocated to a separate bin j . The vector of input conditions is denoted as x_j for a corresponding
 315 bin $j = 1, \dots, B^x$, where B^x is the total number of all bins of all input conditions.

The dimension of x_j is given by the number of input conditions $w = \text{Dim}(X)$. The entire set of input conditions is denoted as $\bar{x} := \{x_j\}_{j=1}^{B^x}$. For each combination of input conditions, a separate operational strategy, i.e., setpoints of the system within the specified system boundaries, $\bar{u} := \{u(x_j)\}_{j=1}^{B^x}$ is defined. The total number of bins B^x is usually defined as a fullfactorial multiplication $B^x = B^{x^{(1)}} \cdot \dots \cdot B^{x^{(w)}}$, where $B^{x^{(i)}}$ denotes the number of bins defined for each condition $x^{(i)}$.

320 2.1.1 Use of frequency distribution for long-term prediction

In order to extrapolate the effects of the input conditions over long periods of time, it is usually made use of a relative frequency distribution $p_{\Delta\tau}$, which is representative of the input conditions within a period $\Delta\tau$. Hence

$$\sum_{j=1}^{B^x} p_{\Delta\tau}(x_j) = 1, \quad (4)$$

which can be scaled to an (absolute) frequency distribution

$$325 h_{\tau}(x) = p_{\Delta\tau} \cdot \tau \quad (5)$$

for a time period

$$\tau = Y \Delta\tau, Y \in \mathbb{N}. \quad (6)$$

For wind turbines, ~~this usually assumes~~ an annual distribution for the wind conditions, i.e., $\Delta\tau = 1$ year, ~~to be~~ is able to represent the variations through the different seasons. With the frequency distribution and the planned operational strategy, a

330 ~~mean-damage-increment-damage~~ $\Delta D_{fm}(\bar{u}, h_{\Delta\tau})$ can then be determined over the period $\Delta\tau$, i.e., an annual damage progress assuming an annual wind distribution. ~~The IEC-standard-approach uses wind and turbulence classes for a type-certification of wind turbines. The wind speeds are modelled through a Rayleigh-distribution for the annual frequency, with a recommended binning-resolution of 1 or 2 m/s for the wind speeds. The turbulence intensity is a fixed, but wind-speed dependent value using a 90% quantile (IEC, 2019). Principally, the choice of the frequency distribution is also part of the system boundaries to be~~
 335 ~~selected and includes a large part of the uncertainties in the long-term planning together with the choice of the relevant external input conditions. An alternative would be to use representative time series data combined with probabilistic approaches for the fatigue damage prediction (Hübner, 2019). Such an approach requires more computational effort and is thus not yet suitable for a condition-based planning approach.~~

Using this and the assumption of a linear damage accumulation, damage can also be defined as a function of τ depending
 340 on the defined frequency distribution over that period and the operational strategy

$$D_{fm}(\tau; \bar{u}, h_{\tau}) := \sum_{j=1}^{B^x} d_{fm}(x_j, u_j) h_{\tau}(x_j) = \underbrace{\sum_{j=1}^{B^x} d_{fm}(x_j, u_j) h_{\Delta\tau}(x_j)}_{\Delta D(\bar{u}, h_{\Delta\tau})} Y. \quad (7)$$

where $d_{fm}(x, u)$ is the damage ~~rate-increment~~ under the external input conditions x and the control setpoints u . It is also possible to compute the energy production accordingly by

$$E(\tau; \bar{u}, h_{\tau}) := \sum_{j=1}^{B^x} P(x_j, u_j) h_{\tau}(x_j) = \underbrace{\sum_{j=1}^{B^x} P(x_j, u_j) h_{\Delta\tau}(x_j)}_{\Delta E(\bar{u}, h_{\Delta\tau})} Y. \quad (8)$$

345 where ~~$P(x, u)$ is the power production~~ $P(x, u) = \frac{E(x, u)}{\Delta\tau}$ ~~is the energy increment~~ under the input conditions and $\Delta E(\bar{u})$ the ~~energy-increment-average annual energy~~ within $\Delta\tau$.

With adapted operational control for modified lifetime, the time period over which energy is produced is changed as well. The total lifetime energy yield can be computed by introducing a lifetime extension factor. It relates the lifetime with the reference operational strategy to the modified lifetime:

$$350 \quad c^{ext} := \frac{\tau^{life}}{\tau^{ref}} = \frac{D_{fm}(\tau^{ref}; \bar{u}^{ref}, h_{\tau})}{D_{fm}(\tau^{ref}; \bar{u}, h_{\tau})} = \frac{1}{D_{fm}(\tau^{ref}; \bar{u}, h_{\tau})} = \frac{\Delta D_{fm}(\bar{u}^{ref}, h_{\Delta\tau})}{\Delta D_{fm}(\bar{u}, h_{\Delta\tau})}. \quad (9)$$

Until now, the resulting lifetime was denoted as τ^{life} , but in fact, this value is computed from damage $D_{fm}(\cdot)$ relevant for a certain failure mode fm and thus also only valid for this specific failure mode. For this reason, it is from now on denoted as $\tau_{fm}^{life}(\bar{u})$ and the extension factor as $c_{fm}^{ext}(\bar{u})$. With this, Eq. (9) can be expressed as

$$\tau_{fm}^{life}(\bar{u}) = \frac{1}{\Delta D_{fm}(\bar{u}, h_{\Delta\tau})} = \frac{\Delta D_{fm}(\bar{u}^{ref}, h_{\Delta\tau}) \cdot \tau^{ref}}{\Delta D_{fm}(\bar{u}, h_{\Delta\tau})} = c_{fm}^{ext}(\bar{u}) \cdot \tau^{ref}. \quad (10)$$

355 The ~~deterministic~~ lifetime extension factor $c_{fm}^{ext}(\bar{u})$ can thus be used to compute the potential for lifetime extension on any time period where the damage increment is compared for two different strategies.

Then, the energy production from the optimized operational strategy \bar{u}^{opt} is given by

$$E\left(\tau_{fm}^{life}(\bar{u}^{opt}); \bar{u}^{opt}, h_\tau\right) = c_{fm}^{ext}(\bar{u}^{opt}) \cdot E\left(\tau^{ref}; \bar{u}^{opt}, h_\tau\right). \quad (11)$$

Within the course of this work, $D_{fm}(\tau^{ref}; \bar{u}, h_\tau)$ is ~~computed in most cases, but it later used within the optimization process.~~

360 It is important to realize that this value is actually closely ~~to~~ related to the ~~damage computed with the~~ reference strategy. This becomes more clear when the damage ~~rate is increments are~~ connected to the fatigue damage budget ~~in the following Sect. 2.2.~~

~~Then, the energy production from the optimized operational strategy \bar{u}^{opt} is given by~~

$$E\left(\tau_{fm}^{life}(\bar{u}^{opt}); \bar{u}^{opt}, h_\tau\right) = c_{fm}^{ext}(\bar{u}^{opt}) \cdot E\left(\tau^{ref}; \bar{u}^{opt}, h_\tau\right).$$

365 Up to now, the assumed damage progression is applicable to any failure mode where damage accumulates over time. With this, we implicitly also assume that the details about material properties of the specific failure mode are included in $d_{fm}(x_j, u_j)$. ~~Since fatigue is a design-driving failure mode and also one for which our proposed method is suited quite well, details for computing the damage rate for fatigue are explained in the following.~~

2.1.1 ~~Damage and DEL calculation~~

370 2.2 ~~Relationship between fatigue damage and damage equivalent load (DEL)~~

Fatigue damage is ~~induced by dynamic load cycles, which act due to forces and bending moments at various places of a turbine. In simplified words, each load cycle leads to a small growth of tiny cracks inside of a material, which ultimately causes the material to break or a component to fail. The crack appears at a very specific location, which is caused by the dynamic loads at that point. Nevertheless, it is not possible to obtain the loads at every single location. Since the weakest failure mode~~ ultimately defines the failure of the system, it is often sufficient to consider only the most important loads at specific locations for simplification. These loads are representatives for the fatigue damage of a material at a specific point like e.g. at the blade root perpendicular to the rotor plane (Manwell et al., 2011). Within this section, the accumulation of damage for arbitrary failure modes under various deterministic external conditions is explained and related to the standard approach for counting load cycles and fatigue damage calculation. This is ~~typically~~ based on the assumption of a linear damage accumulation by 380 Palmgren and Miner (Miner, 1945). The high uncertainties resulting from this approach, especially for wind turbine rotor blades but also for other components, is well known for a long time (Sutherland, 1999). In particular, it is not possible to consider sequence effects of loads on the damage. Also, the material properties of composite materials can only be covered to a small extent by this approach. As it was also mentioned in the literature study (Sect.1.1), estimating the state-of-health of different wind turbine components is still a challenging task for future research. Despite that, it remains common practice 385 to use linear damage accumulation for structural components of wind turbines. Especially for the comparison of loads under different environmental conditions or control approaches, it remains a useful approach as a first step, before more advanced evaluations can be examined with further development.

For the explanation of the general process, the failure mode index fm is dropped. The fatigue damage ~~rate-of-a-time-series~~ increment of a load time series simulated on the seconds scope, with input conditions x_j , is given by

$$390 \quad d(x_j, u_j) = \sum_{i=1}^{n_{cyc,j}} \frac{n_{ij}}{N_{ij}} \quad (12)$$

for i effective load collectives with a number of load cycles n_i . N_i denotes the maximum bearable number of load cycles until failure for the corresponding specific oscillation amplitude. The number of load cycles counted in the load time series of length Δt is denoted with $n_{cyc,j}$. The tolerable number of load cycles N_{ij} depend on D^{ult} and can be determined with

$$N_{ij} = \left(\frac{D^{ult}}{L_{ij}} \right)^m \quad (13)$$

395 L_{ij} represents the oscillation amplitude of a load cycle and are usually obtained from a rainflow counting algorithm. The parameter m is the component specific Wöhler exponent describing the slope of the S-N curve as negative inverse on a double logarithmic axis. In the formulation of Eq. (13), the mean load is neglected and no Goodman correction is performed. The value D^{ult} denotes the ultimate design load which would lead to a damage of $D = 1$ if it occurred once. Therefore, D^{ult} is a design parameter which needs to be determined from the design process under consideration of all conditions and their
400 frequency for the desired reference design period τ^{ref} . In addition, it normally includes safety margins and design reserves. For simplification ~~D^{ult}~~ D^{ult} can be scaled in such way, that

$$D(\tau^{ref}; \bar{u}^{ref}, h^{ref}) = 1 \quad (14)$$

is valid, i.e. that fatigue damage is fully utilized with the reference operational strategy and under some site specific reference frequency distribution

$$405 \quad h^{ref}(x) := h_{\tau^{ref}}(x) = p_{\Delta\tau} \tau^{ref} \quad (15)$$

In this case, ~~D^{ult}~~ D^{ult} can be expressed by making use of the damage equivalent fatigue load (DEL). It is a representative value which would yield the same damage as the considered time varying signal with a constant amplitude and frequency. This value is referred to an equivalent number of load cycles N^{eq} . Then, the short-term DEL is computed by

$$DEL_{\sim}^{st,st}(x_j, u_j) = \left(\frac{\sum_i n_{ij} (L_{ij})^m}{N^{eq}} \right)^{\frac{1}{m}} \quad (16)$$

410 and the total DEL over the time span τ is given by

$$DEL(\tau; \bar{u}) = \left(\sum_{j=1}^{B^x} (DEL^{st}(x_j, u_j))^m (h_{\tau}(x_j)) \right)^{\frac{1}{m}} \quad (17)$$

This can be used to solve Eq. (14) for D^{ult} :

$$\begin{aligned}
1 &= \sum_{j=1}^{B^x} d(x_j, u_j^{ref}) h^{ref}(x_j) = \sum_{j=1}^{B^x} \sum_i^{n_{cyc,j}} \frac{n_{ij}}{N_{ij}} h^{ref}(x_j) \\
&= \sum_{j=1}^{B^x} \sum_i^{n_{cyc,j}} \frac{n_{ij} (L_{ij})^m}{(D^{ult})^m} h^{ref}(x_j) = \sum_{j=1}^{B^x} \underbrace{\left(DEL^{st}(x_j, u_j^{ref}) \right)^m}_{DEL(h^{ref}; \bar{u})^m} h^{ref}(x_j) \frac{N_{eq}}{(D^{ult})^m}
\end{aligned}$$

$$415 \Rightarrow D^{ult} = DEL(h^{ref}; \bar{u}^{ref}) (N_{eq})^{\frac{1}{m}} = DEL^{ref} (N_{eq})^{\frac{1}{m}} \quad (18)$$

This can subsequently be inserted to Eq. (13) so that the damage can be expressed using the DELs as a relative value

$$d(x_j, u_j) = \sum_i^{n_{cyc,j}} \frac{n_{ij}}{N_{ij}} = \frac{n_{ij} (L_{ij})^m}{(DEL^{ref})^m (N_{eq})} = \frac{DEL^{st}(x_j, u_j)^m N_{eq}}{(DEL^{ref})^m N_{eq}} = \left(\frac{DEL^{st}(x_j, u_j)}{DEL^{ref}} \right)^m \quad (19)$$

In order to model the non-linear damage rate-increment for the external conditions, surrogate models can be created by using the relationship to the short-term DELs which is given by equation (19). In principle, surrogate models for the damage rates
420 increments could directly be computed, but building up the models for the DEL is more common and easier to interpret because the Wöhler-exponent m adds additional non-linearity to the damage value.

~~Having determined the basic relationships between all of the required quantities for the fatigue damage progression, the theoretical background for all of the four identified steps can be explained, starting with the setpoints for the real-time controller.~~

425 2.3 **Step 1: Provide adaptable real-time controller of the wind turbine**

3 Definition of example system and implementing prerequisites for optimization

Comment to reviewers

This section contains content of several previous sections and now summarizes all prerequisite steps.

- Section 3.1 contains the main content of previous Section 4.
- Section 3.2 combines the content of previous Sections 2.2 and 4.1. The text is also significantly shortened.
- Section 3.3 combines the content of previous Sections 2.3 and 4.2. The text is also significantly shortened.

4 **System definition for application example: One turbine in a small regular-grid wind farm**

~~The presented method for optimal planning is applied to the demonstration example. Before the four steps can be applied~~
430 Based on the theoretical background for fatigue calculation, the four step process will be applied to a specific use case. Therefore, the system boundaries need to be determined.

~~In our application example, we for the exemplary use case will be defined at first. Afterwards, the first two steps of the process are explained and applied to the example.~~

3.1 ~~System boundaries for application example~~

435 ~~We want to focus on optimal operation of a single turbine within a wind farm. This means ,that although our system boundary is well-defined around the single turbine, that~~ effects from the surrounding wind farm have to be taken into account as well. These include mainly the wake effects from other turbines, which act on the considered turbine and are, under normal operation, a ~~main-significant~~ driver of its loads. Each single considered turbine will thus be able to react to the wake effects from the surrounding turbines, but the effect from changes in control on the wake cannot be considered yet. ~~How to address this issue and other shortcomings and potential improvements of the approach will be discussed in Sect. ??.~~

3.1.1 ~~Modelling of single turbine and its system boundaries~~

The ~~example wind farm consists of 9 turbines with a regular 3×3 layout, shown in figure 5a. The turbine spacing is 8 rotor diameters in x direction and 4 rotor diameters in y direction. This example farm was already used in Schmidt et al. (2021). The generic direct-drive wind turbine IWT7.5 with a nominal power of 7.5 MW, rotor diameter of 164 m and a hub height of 100 m~~ is used (Popko et al., 2018). ~~Layout of example wind farm~~

3.2 ~~System boundaries for considered system: Modelling of single turbine~~

~~The system boundaries for the single turbine are defined by the selected external input conditions, i.e. the definition of X , the utilized aero-elastic model for the simulation of loads. In addition, the failure modes need to be selected and the damage rates with their specific parameters need to be computed from the loads.~~

450 3.1.1 ~~Computation of turbine loads~~

To compute the loads of the turbine ~~on the so-called seconds scope ($\Delta t = 0.01s$)~~, the aero-elastic load simulation tool "The Modelica library for Wind Turbines" (MoWiT) (Thomas, 2022) is employed. Three-dimensional wind fields covering the properties of the external conditions within for simulation ~~is-are~~ used as input. They are created with the software Turbsim (Jonkman, 2009).

455 3.1.1 ~~Selected external environmental input conditions~~

~~For the application of optimal planning in this paper, two-MoWiT is developed at Fraunhofer IWES as an object-oriented library for fully-coupled aero-hydro-servo-elastic simulations of wind turbines. Detailed information on the development of MoWiT can be found in the literature (Thomas et al., 2014; Leimeister and Thomas, 2017). The tool covers on- and offshore turbines, with bottom-fixed substructures and also floating wind turbines. It is coupled to the adaptable controller outlined in Sect. 3.2. Two~~ major environmental inputs influencing the wind turbine loads in power production mode are considered as local

input conditions: mean wind speed v and turbulence intensity at hub height TI . Those input conditions are defined locally as the inflow to a single turbine which positioned its rotor perpendicular to the main inflow wind direction. All other parameters which define the inflow wind field, such as vertical and horizontal wind shear are fixed at their IEC-standard values. The local inflow on a turbine from wake effects is covered through an increase in turbulence intensity only and does not include wake meandering effects. This simplification allows splitting the aero-elastic turbine simulations from the wake modelling, and thus reduces simulation effort. ~~The range of simulated data will be defined in Sect. ?? where the surrogate models for the example is built up.~~ Considering other effects like wake meandering for the creation of surrogate models is possible through an extension of the load simulations but goes beyond the scope of this work because the major effect of an increase in loads is covered through the applied approach.

470 3.1.1 Selected failure modes

For the demonstration of the approach, the structural loads of the blades and the tower are considered. Both are supposed to last for the complete design lifetime of 20 or 25 years. Both are also influenced by the turbine controller and the wake induced turbulence. For the blades, the flapwise and edgewise bending moments (bm)³ are considered as separate failure modes, because they represent the two major load driving moments on the rotor blades. ~~The distribution of moments along the blade root is not fully reflected by this approach, but it is possible to cover the differing effects which influence both moments. While the edgewise bm is mainly driven by the gravitational loads of the rotating system, the flapwise bm is strongly influenced by the turbulence and thus from the wake effects.~~ For the tower, the combined bending moment at the bottom is utilized as failure mode. ~~This is dominated by the fore-aft movement of~~ All these loads can be considered as representatives for the fatigue accumulation of different components that can be influenced by the wind turbine controller and the environmental conditions in different ways. ~~While the tower and the flapwise bending moment are more strongly influenced by turbulence, the tower. The direction of the fore-aft moment actually depends on the wind direction, since the coordinate system is always defined with respect to the rotor plane perpendicular to the main wind direction. Therefore, the use of the combined moment also neglects some influencing factors, but still represents the influence on the tower fatigue loads sufficiently well for demonstration~~ variations in the edgewise bm are driven by gravity loads dependent on the rotor speed, i.e. the controller and the wind speed.

485 The considered loads, their corresponding abbreviations and the utilized Wöhler-exponent m are summarized in Table 1. ~~For the blades, an exponent of $m = 10$ is selected, which is a common choice for representing the blade root laminate.~~ Using linear fatigue accumulation by using DEL is a very strong simplification for the fatigue degradation of laminate, which is a composite material containing fibre glass. Using this approach is still standard for design calculation and allows for a straight forward use without detailed knowledge about the material properties. For the tower, an exponent of $m = 3$ is used, which is ~~representative for steel components and $m = 10$ for the blade loads as an approximate for fibre~~ (Sutherland, 1999). ~~In total, the three selected failure modes are representatives for the fatigue accumulation for different components in the wind turbine and therefore applicable for the demonstration of the optimal planning approach.~~ glass (Sutherland, 1999).

³bending moments are abbreviated with bm from this point onwards

Table 1. Summary of terms for the selected failure modes

Load	Flapwise Bending Moment	Edgewise Bending Moment	Tower Bottom Bending Moment
Abbreviation	Flapwise bm	Edgewise bm	Tower (bottom) bm
Wöhler Exponent	10	10	3
Short-Term DEL	$DEL_{flap}^{st}(x, u(x))$ [Nm]	$DEL_{edge}^{st}(x, u(x))$ [Nm]	$DEL_{tower}^{st}(x, u(x))$ [Nm]
Damage Rate	$d_{flap}(x, u(x))$ [1/h]	$d_{edge}(x, u(x))$ [1/h]	$d_{tower}(x, u(x))$ [1/h]

3.2 From surrounding system to considered system: From wind farm to turbine

~~Since the frequency distribution of the wind direction has a major influence on how often a turbine is affected by~~

495 3.1.1 Wind farm setup: From surrounding system to considered wind turbine

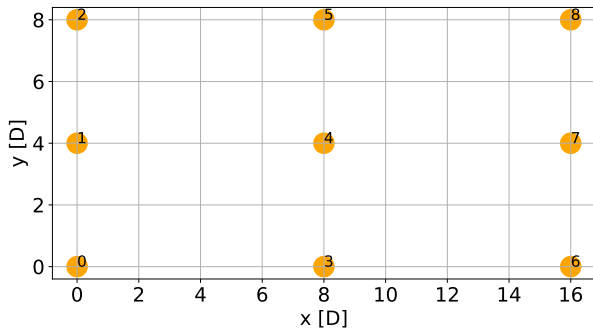
The influences of the surrounding system on the considered wind turbine are covered by a site-specific wind distribution and the wake influences from the surrounding turbines in the wind farm. The wind farm consists of 9 turbines with a regular 3×3 layout, shown in Fig. 5a.

It was already used in Schmidt et al. (2021). Within this work, we optimize operational strategies for the turbine in the
500 centre (index 4). Doing so, we can put a focus on the method for operational planning and the discussion of derived results.
There are various studies and models to illustrate the effects of wakes on the loads ranging from wake meandering to partial
wake effects (Mendez Reyes et al., 2019; Nash et al., 2021). Since the core of this work lies on the optimization methods, we
limit ourselves here to a simple steady-state modelling of the wake effects for wind and turbulence which cannot cover these
505 effects yet. For this purpose we use the IWES software FOXES (Schmidt, 2022). The local wind speed is computed using
the Gauss-type wake model by Bastankhah and Porté-Agel (2016). The wake-induced TI is calculated using the wake of other
turbine, it needs to be considered for an optimal planning of damage. Therefore, a site-specific wind distribution is required
to cover the influences of the surrounding system. The global wind conditions need to be transferred to local input conditions
for the considered system, i.e. the single wind turbine. This is done by using a basic steady-state wake model, which transfers
from ambient wind speed and wind direction to local top-hat wake model as described in IEC (2019). For the ambient TI,
510 we use the wind-dependent Weibull distribution according to IEC (2019) with class B at the 50% quantile to cover the mean
effects at such a site. For the superposition of wakes, we use a linear superposition for the wind speed and TI. At first, the
maximum superposition for TI. Local TI depending on the ambient wind data is defined before the wake model is briefly
explained and a local wind speed and direction is shown in Fig. 5b.

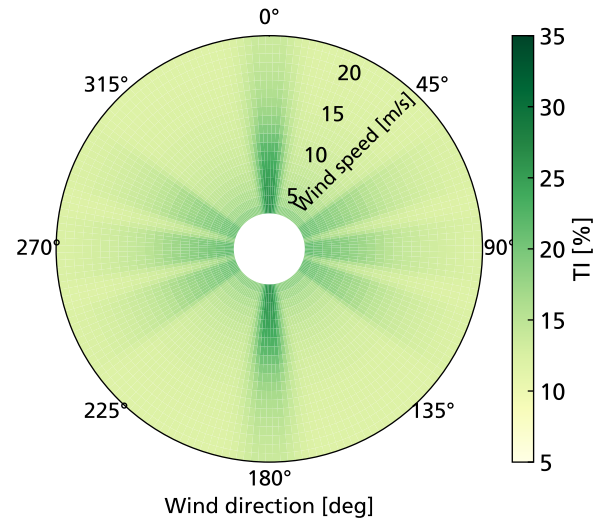
The annual frequency distribution is derived from both.

515 3.1.2 **Global wind conditions (Ambient Wind Data)**

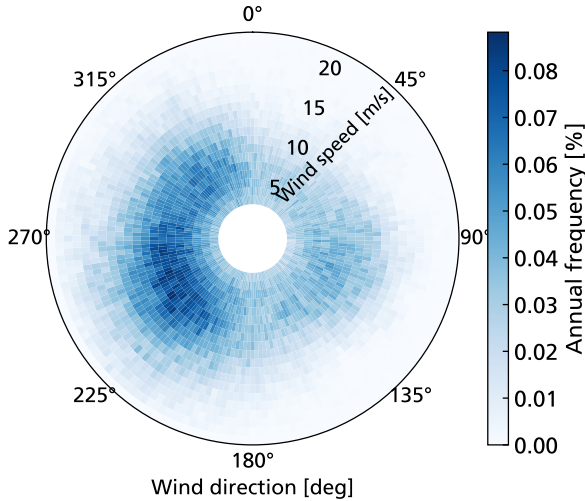
ERA5 data representative of a wind farm a 30-year time series of ERA5 data in the North Sea are used (Hersbach et al., 2018).
From the time series, a 30-year period from 1990 to 2019 with a resolution of 1h, the from 1990 to 2019 (Hersbach et al., 2018)



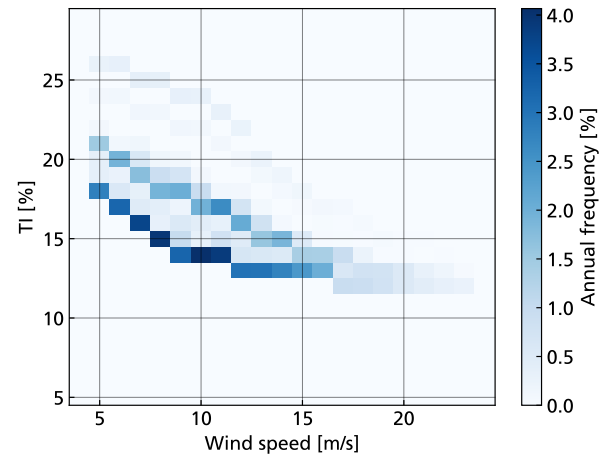
(a) Farm layout (distance in rotor diameters D)



(b) Local TI for considered turbine (including wake effects)



(c) Relative annual frequency for each combination of wind speed and direction



(d) Relative annual frequency for each combination of wind speed and TI (including wake effects)

Figure 5. [Setup for surrounding system of the wind turbine](#)

Comment on figure

Figure 5 is new to clarify the binning process

The mean wind speed and wind direction at 100 m height is-are extracted to create a relative frequency distribution of ambient wind speed \bar{v}^{amb} and wind direction $\bar{\theta}^{amb}$, which are both subdivided into bins. ~~This relative distribution is representative for~~

520 ~~a one-year period.~~ Therefore, the reference relative wind distribution for the ambient wind conditions is $\mathbf{p}_{\Delta\tau}^{ref}(\bar{v}^{amb}, \bar{\theta}^{amb})$ with $\Delta\tau = 1\text{year}$ ~~$\Delta\tau = 1\text{ year}$.~~ Because wind speed and direction are covered separately, the total number of bins B^x is subdivided into bins for each direction. The wind speeds \bar{v}^{amb} are first binned with a resolution of 1 m/s from 1.5 to 49.5 m/s. ~~Afterwards, the values below 4.5 m/s and above 23.5 m/s are removed (Number~~ Only values within the operating envelope of the turbine ~~(4.5m/s $\leq v^{amb} \leq 23.5\text{m/s}$, number of wind speed bins $B^{v^{amb}} = 20$).~~ ~~This implies that the turbine is assumed to be in idling mode below and above these values. Therefore, values between these two wind speeds, where derating actually does have an influence on,~~ where derating can influence the turbine, are considered for optimization. It also means that $\mathbf{p}_{\Delta\tau}^{ref}(\bar{v}^{amb}, \bar{\theta}^{amb})$ does not sum up to 1 anymore, ~~but to 0.9.~~ The wind direction is binned with a resolution of 2° from 0° to 358° (Number of wind speed bins $B^{\theta^{amb}} = 180$). This results in a total number of $B^{x^{amb}} = 180 \cdot 20 = 3600$ bins. The ~~ambient turbulence intensity is not available from the ERA5-data. It is modelled as a fixed value, and is set to 5% for all wind speeds and wind directions.~~ percentage annual frequency for those bins is shown in Fig. 5c.

530 ~~Within the system boundaries of the application example, we concentrate on the additional TI from wake. Other external inputs like e.g. atmospheric turbulence or temperature are outside the system boundaries and implicitly considered as fixed values.~~

3.1.2 Wake modelling

To compute the wake effects, the IWES software FOXES⁴ is used. More details on the software can be found in ~~(Schmidt et al., 2021).~~ In this case, only a small part of the software is used to compute the steady-state wake effects for each of the turbines under the reference conditions. From the view of For a single turbine, the wake model represents a function which maps the ambient mean wind speed v^{amb} and wind direction θ^{amb} to the local mean wind speed v and turbulence intensity TI is required. ~~From the view of a specific turbine, the wake modelling function depends on number, distance and also operation of the surrounding turbines. Thus, the wake function is valid separately for each turbine $s = \{1, \dots, S\}$ in a wind farm with S turbines and denoted as $f_s^{wake}(v^{amb}, \theta^{amb})$.~~ The local wind speed is computed using the Gauss-type wake model by Bastankhah and Porté-Agel (2016). ~~The wake induced turbulence intensity is calculated using the top-hat wake model as described in IEC (2019).~~

540 ~~The wake induced turbulence intensity is calculated using the top-hat wake model as described in IEC (2019).~~

3.1.2 Local frequency distribution

For computing the damage and energy production with the frequency distribution of the ambient wind conditions defined above, the wake modelling function needs to be included in equations (7) and (8). For clarification, the sum over B^x which was formerly used is now subdivided into two separate sums over the specifically defined input conditions.

545 ~~above, the wake modelling function needs to be included in equations (7) and (8). For clarification, the sum over B^x which was formerly used is now subdivided into two separate sums over the specifically defined input conditions.~~

This implies for a turbine s :

$$\underline{D_{fm}(\tau; \bar{u})} = \sum_{j=1}^{B^{v^{amb}}} \sum_{i=1}^{B^{\theta}} d_{fm}(f_s^{wake}(v_j^{amb}, \theta_i^{amb}), u((v_j^{amb}, \theta_i^{amb}))) h^{ref}(v_j^{amb}, \theta_i^{amb})$$

⁴The software was formerly named flappy, and version v0.4.3.3 was applied.

and

$$550 \quad \underline{E(\tau; \bar{u})} = \sum_{j=1}^{B^v} \sum_{i=1}^{B^\theta} P(f_s^{wake}(v_j^{amb}, \theta_i^{amb}), u((v_j^{amb}, \theta_i^{amb}))) h_s^{ref}(v_j^{amb}, \theta_i^{amb}).$$

As explained in Sect. ??, the number of external wind condition bins determine the number of optimization variables. Reducing those can thus reduce the effort for optimization. Since the interaction of the turbines is only modelled unidirectional, without considering the influence of the changing-changed control setpoint on the wake of wake towards other turbines, it is possible to create a local frequency distribution for each turbine, which only depends on the distribution of local wind speeds and turbulence. To do so, the frequencies of $\mathbf{p}_{\Delta\tau}^{ref}(v^{amb}, \theta^{amb})$ are binned again into $B^v = 20$ wind bins, as before, and $B^{TI} = 25$ TI bins with a width of 1% starting from 5%, resulting in 500 total bins. ~~D~~The frequency distribution for the additional binning is denoted as \tilde{h}_s^{ref} , and is only valid separately for each turbine ~~s: s = {1, ..., S}~~ s: s = {1, ..., S} in an arbitrary wind farm with S turbines. The local frequency distribution of the centre turbine 4 is shown in Fig. 5d. The TI-values increase from the ambient TI, which still shows the highest relative frequency. The frequency of TI values increases for certain combinations as indicated from Fig. 5b. Then, the damage and energy calculation ~~from equations (??) and (??) can be simplified to~~ can be derived:

$$560 \quad \tilde{D}_{fm}(\tau; \bar{u}) = \sum_{j=1}^{B^v} \sum_{i=1}^{B^{TI}} d_{fm}(v_j, TI_i, u(v_j, TI_i)) \tilde{h}_s^{ref}(v_j, TI_i). \quad (20)$$

and

$$565 \quad \tilde{E}(\tau; \bar{u}) = \sum_{j=1}^{B^v} \sum_{i=1}^{B^{TI}} P(v_j, TI_i, u(v_j, TI_i)) \tilde{h}_s^{ref}(v_j, TI_i). \quad (21)$$

This simplified form ~~will thus,~~ which adds uncertainty to the optimization result, will be used in the results part ~~where the approach is applied. From the additional binning, additional uncertainty is added to the results. This is however neglectably small. It is also possible to use equations (??) and (??) directly for the optimization, with a higher computational time during application of our approach. The uncertainty can be influenced by the number of bins selected. It can be well estimated in comparison to the original binning and lies below 1% for the considered cases.~~

570 **3.2 Adaptable real-time controller of the wind turbine (Step 2: Build surrogate models for damage progression and energy production1)**

The primary objective of a wind turbine controller is to maximize power production while meeting the requirements of a grid operator (Burton et al., 2011; Njiri and Söffker, 2016; Requate et al., 2020). Additionally, secondary objectives such as load reduction are pursued during control design. This can be achieved e.g., by implementing features for reduction of loads on specific components. Examples are exclusion zones to reduce tower vibrations or individual pitch control (IPC) to reduce fluctuations in blade root bending moments. However, these secondary objectives usually force the controller to deviate from

optimal operation with regard to its primary objectives. Some secondary objectives might even compete with one another, e.g., blade root loads and pitch actuator activity for IPC. We now assume that the balance between primary objective and secondary objectives can be selected externally by adapting the controller through a control setpoint.

580 In Sect. 2.1, we already introduced the control setpoint as $u(x)$ ~~is introduced as~~. We assume this to be an abstract value which can be selected based on the external input conditions x . ~~This means~~ Thus, u is ~~basically~~ a vector of ~~different setpoints sent to the real-time controller~~ controller setpoints, which in turn reacts by adjusting its own internal parameters. ~~The exact effect that the setpoints have on system behavior strongly depends on the system at hand. Taking~~ In a larger wind farm system, which is composed of multiple turbines, which uses wake steering or ~~reduction as an example~~ wake reduction, $u(x)$ ~~would be~~
585 ~~the open-loop setpoint for the~~ could be the yaw angle or the amount of ~~derating of the turbine depending on wind speed and wind direction (Nash et al., 2021). To discuss the way in which u can be integrated into an optimal planning approach,~~ power derating (Nash et al., 2021).

Within the remainder of this paper, we assume a one-dimensional control setpoint for the power derating of a little more background information on the control design of wind turbines is given, before methods for derating are presented ~~controller setpoints of choice within this work.~~ single turbine. This is a commonly available input, as reduced power capability is also requested by grid operators to mitigate grid congestion.

~~For wind turbine controller design, the trade-off between various objectives needs to be found. Load reduction or mitigation of various components or specific failure modes competes with the influence of high control activity on actuators or other failure modes. The main objectives remain reliably producing energy while at the same time meeting the requirements of a grid operator (Burton et al., 2011; Njiri and Söffker, 2016; Requate et al., 2020). Due to the varying influence of external conditions and the acro-servo-hydro-dynamic coupling of all the failure modes, the selection of a trade-off depends on multiple individual factors for each turbine. When aiming at adaptive operation, multiple control setpoints need to be selected so that each of them prioritizes a different objective or a combination of such. Due to the strong influence of the external conditions (mainly wind conditions) on the wind turbine performance, an individual trade-off for each of the various conditions might actually be~~
590 ~~required.~~

~~Therefore, providing an adaptable real-time controller definitely possible in many ways for wind turbines. Through a preselection of control setpoints, one can reduce the computational effort and use them for simulations to built up surrogate models. Since derating can also be applied to any existing turbine and has the ability to reduce fatigue damage, it is selected as an instrument for the planning of damage progression in this work. Also, the conflict to the energy production of the individual turbine is directly clear. The derating of a turbine can be performed in several ways, and the specific method will have a large influence on the load reduction.~~ There are several studies which investigate derating methods with respect to ~~their influence on various objectives~~ like various objectives. These include power regulation for the grid (~~ancillary services~~), wake reduction (~~power maximization~~) or loads. In Houck (2022), several studies on derating (or axial-induction control) are summarized and sorted into the mentioned categories. Many studies investigate load reduction as a side effect, while the main objective is either
605 ~~the power regulation or reducing the wake on the downstream turbine. For the discussion of derating methods, one has to distinguish between the partial and the full load region of a wind turbine controller. Below the rated wind speed, the dominant~~

615 goal in normal operation is to obtain the maximum available power from the wind. In the full-load region, the generator speed is held constant by pitching the blades and the turbine operates at its rated generator torque and power. The partial load region, where maximum power point tracking (MPPT) is applied, is also referred to as region 2 and the full-load region above rated wind speed as region 3. The MPPT in partial load is obtained by operating the turbine at the maximum value of the power coefficient c_p , which is a function of the tip-speed ratio λ and the pitch angle β . Therefore, the power can be reduced by adapting either of them or both. Benefits and shortcomings of different approaches have been applied and investigated in various studies (Zhu et al., 2017; Astrain Juangarcia et al., 2018; Lio et al., 2018; Meng et al., 2020). For the reduction of wake effects, minimizing the thrust is beneficial, but it can have negative effects on tower loads when the rotor speed reduction leads to resonance effects (Meng et al., 2020). In Astrain Juangarcia et al. (2018) similar load reducing effects were observed when the tip speed ratio was held constant (so called constant- λ -method) and when thrust was minimized. Overall, the studies show that the setpoints need to be selected specifically for each turbine and objective.

625 In the full load region, the torque set point is normally reduced for derating. It allows for a fast recovery of power when derating is no longer required, and is thus beneficial for ancillary services (Fleming et al., 2016; van der Hoek et al., 2018). However, it only has a minor effect on the fatigue loads of the blade and the tower. Reducing the generator speed mainly has a strong positive effect on the blade loads in flapwise direction (Requate and Meyer, 2020), while reducing the torque has a positive influence on the driving torque loads (Pettas et al., 2018). The effect on the tower loads are quite turbine dependent because a reduction in generator speed can reduce oscillations to some extent but often also increases them due to the lowered aerodynamic damping (van der Hoek et al., 2018). Therefore, a mixed method between reducing torque and speed might be advantageous, again depending on individual objectives and turbine characteristics.

630 Concluding this step, it is evident that adaptable real-time controllers already exist for wind turbines, but choice of a specific method is crucial for the use under Within the system boundaries of the planning. In Sect. ??, a specific method is implemented for the application example. The setpoint is then used as one of the inputs for a surrogate model.

635 While derating was already defined as suitable choice for load reduction, the implementation of specific setpoints of the real-time controller still needs to be specified. The IWT7.5 is controlled with the IWES research controller developed internally in Matlab Simulink (Wiens, 2021). It implements a standard torque-pitch controller of a wind turbine (see e.g. Burton et al. (2011) or Njiri and Söffker (2016)). In region 2, the $k\omega^2$ -law is applied to set the generator torque M . The coefficient k is derived from the aerodynamic characteristics of the turbine, with the standard approach to achieve MPPT. In region 3 the turbine operates at its rated power P_r . Here, a PI-controller for keeping the rated generator speed ω_r constant by pitching the blades is implemented. The generator torque is fixed to its rated value M_r . The transition between region 2 and 3 is simply determined by a linear relationship between torque and speed, which starts from 95% of ω_r .

645 ~~Within the sytem boundaries of~~ this study, the main objective is not to determine the best fitting derating method for the generic wind turbine, but to show the benefits of using derating for an optimal planning. Therefore, the choice was is conducted based on the findings from ~~the cited~~ literature and from previous experience with the generic IWT7.5 wind turbine and not through an extensive study and tuning of the controller under various conditions. Also, no additional features like individual pitch control or active dampers are activated. For a real-world application, fine-tuning the controller for every derating

configuration would be beneficial and could lead to an improved performance with respect to loads and power. ~~For showing the benefits of the optimal planning approach, such a fine-tuning is not yet required. The presented derating method represents one potential choice for the derating of a turbine by a proportional factor in all regions, and thus a trade-off between the induced fatigue damage and power production.~~

The IWT7.5 is controlled with the IWES research controller (Wiens, 2021). The derating method is ~~thus~~ implemented such that it reduces power in partial and in full load by a percentage factor $\delta_P \in [\delta_P^{min} = 50\%, 100\%]$. Such a derating method is referred to as proportional delta control in Elorza et al. (2019) or percentage reserve in van der Hoek et al. (2018). ~~By using a single derating factor $u(x) = \delta_P$ as a setpoint for the real-time controller, the combination of a derating method with the creation of surrogate models and the use for the nonlinear optimization is facilitated. It is defined as percentage power factor $\delta_P \in [\delta_P^{min}, 100\%]$. The structural fatigue loads of both, the blades and on the tower should be reduced. A derating down to 50% is considered as sufficient for this purpose, i.e. $\delta_P^{min} = 50\%$.~~

In full load operation, ~~the main goal is to reduce the fatigue loads of the flapwise bm while not increasing or slightly decreasing the tower bm fatigue. In~~ partial load, both tower and blade fatigue loads should be decreased. To do so, the ~~so-called~~ constant- λ method is implemented (Astrain Juangarcia et al., 2018), because we expect a positive effect on these loads based on the literature, and we avoid potential negative effects like a near-stall operation as e.g., by using the minimum-thrust strategy. This is achieved by finding the steady-state pitch angle β so that the reduced power coefficient $\delta_P c_p$ is found while λ is kept constant. From these values, the ~~coefficient k^d for the parameters for~~ derated operation can ~~again~~ be computed.

In region 3, a combined method for reducing the rated generator torque M_r and ω_r is selected. At first, the full load region, ~~the percentage power reduction factor $\delta_P \in [\delta_P^{min}, 100\%]$ is defined to compute the reduced-rated power by-~~

$$\underline{P_r^d = \delta_P P_r.}$$

The reduction factor for the rated generator speed $\delta_\omega \in [\delta_\omega^{min}, 100\%]$ is then defined with a quadratic relationship to the reduction in power by-

$$\underline{\delta_\omega = \delta_\omega^{min} + (1 - \delta_\omega^{min}) \left(\frac{\delta_P - \delta_P^{min}}{1 - \delta_P^{min}} \right)^2}$$

so that the derated generator speed is given by-

$$\underline{\omega_r^d = \delta_\omega \omega_r}$$

and the generator torque by-

$$\underline{M_r^d = \frac{\delta_P}{\delta_\omega} M_r.}$$

In this case, we use $\delta_\omega^{min} = 80\%$. Using this approach, we aim at strongly reducing fatigue loads on the flapwise bm ~~through~~ torque set point is normally reduced for derating. This allows for a fast recovery of power when derating is no longer required, and is thus beneficial for ancillary services (Fleming et al., 2016; van der Hoek et al., 2018). However, it only has a

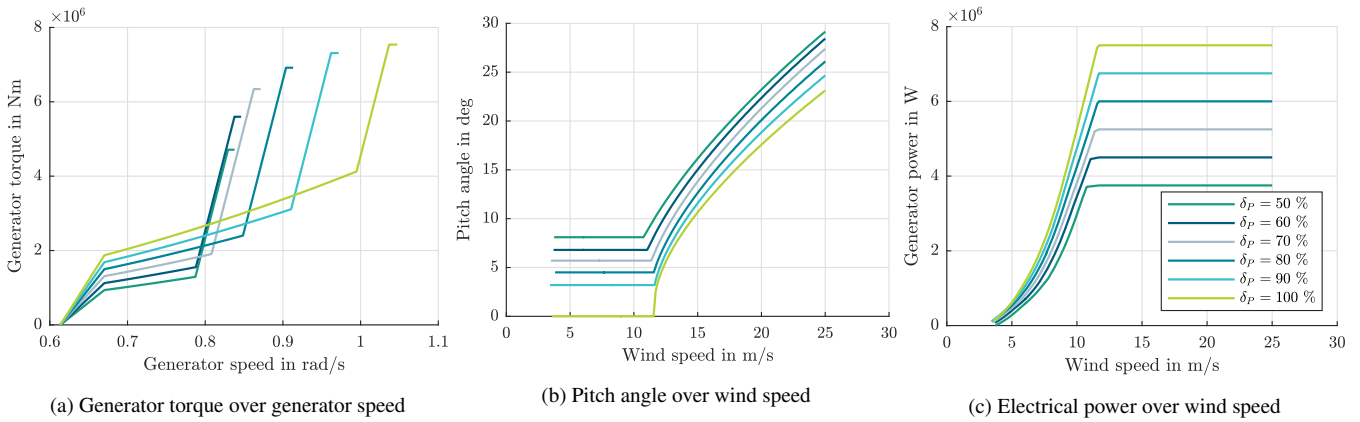


Figure 6. Operating points of the real-time controller for selected derating methods

Comment on figure

Colors of figure 6 are updated

minor effect on the fatigue loads of the blade and the tower. Reducing the generator speed mainly has a strong positive effect on the blade loads in flapwise direction (Requate and Meyer, 2020), while reducing the torque has a positive influence on the driving torque loads (Pettas et al., 2018). The effect on the tower loads are quite turbine dependent because a reduction in generator speed while still providing sufficient aero-dynamic damping on the tower. For the transition region between region 2 and region 3, the slope of the linear transition function was kept constant can reduce oscillations to some extent but often also increases them due to the lowered aerodynamic damping (van der Hoek et al., 2018). Therefore, a mixed method between reducing torque and speed might be advantageous, again depending on individual objectives and turbine characteristics. Both methods are combined for reducing the rated generator torque M_r and ω_r .

In Fig. 6, the operating points of the controller for the selected setpoints are presented. Figure 6a shows the speed-torque curve of the controller. The end point of the curves always determines the combination of M_r and ω_r , so that the process of these point reflects the relationship from Eq. (??) to Eq. (??) in region 3. In region 2. By comparing the progression of these curves, the effect of both strategies can be observed. In partial load, the constant- λ strategy determines a specific combination of the factor k_{ctrl}^d and the parameters including the static pitch angle. The value for k^d is reduced with decreasing δ_P , as it can be seen from the quadratic part of the speed-torque-curves in Fig. 6a. The steady-state operating points of the pitch-angle are plotted over the wind speed in Fig. 6b. The pitch angle in region 2 is kept constant below the rated wind speed for all of the setpoints for the percentage power. The constant value increases with decreasing δ_P . Above rated wind speed, the change of the derived setpoints for the rated generator speed and torque also results in an increasing steady-state pitch angle of the PI-controller. In combination, this results in the steady-state power curves which are shown in Fig. 6c.

695 In order to study the controller under various conditions, the evaluation of aero-elastic load simulations is required. Those load simulations are also used as an input for the surrogate models. Therefore, the selected approach and the results of surrogate models are presented first before the influence of the control setpoints on the DELs of the selected failure modes are discussed

The control setpoints can then be used as optimization variables in the formulation of a mathematical optimization problem. However, using them directly within an optimization requires the full simulation of respective load cases, which is not feasible due to the required computational effort. Instead, surrogate models can be setup which abstract the whole turbine-controller interaction.

3.3 Surrogate models for damage progression and energy production (Step 2)

In order to cover the influence of the various influences of external conditions and control on the fatigue damage, surrogate models have gained growing research interest. The approaches for surrogate modelling, sometimes also called meta-modelling, fatigue damage. They have in common that aero-elastic simulations are used to create a database of fatigue loads for various input conditions. Subsequently, a mathematical model is trained to represent the complex relationship of inputs to the fatigue of different load representatives with a simplified mathematical model. Usually, In Fig. 4, those aero-elastic simulation models are denoted more generally as *higher fidelity models* on the seconds scope. The surrogate model is created by performing multiple simulations for a pool of input samples. Due to the relationship between damage increments and DELs, the short-term damage equivalent loads of different load signals and the electrical power are considered as output quantities as these are most commonly used for fatigue design calculations because it allows to integrate the influence of various external conditions in the design process. A good overview of different surrogate methods and a comparison of their performance is given in Dimitrov et al. (2018). Apart from linear interpolation or polynomial regression, the most popular methods, which are being used for the investigation of surrogates, are gaussian regression (often referred to as Kriging), polynomial chaos expansion and artificial neural networks (Dimitrov, 2019; Hübler, 2019; Slot et al., 2020; Gasparis et al., 2020; Debusscher et al., 2022; Singh et al., 2022)].

Depending on the purpose, a trade-off between accuracy, interpretability, training time, number of required samples and also evaluation time needs to be found, and a method is selected accordingly. All of them need to deal with the uncertainties due to the stochastic nature of the wind, which is also reflected in the fatigue damage and the DELs. Bossanyi (2022) uses a different approach for creating the surrogates by splitting up the inputs into deterministic and stochastic influences.

To be able to use the short-term damage for optimization, it is required to apply a surrogate model because the damage rate needs to be evaluated with a low computational time for an arbitrary combination of inputs. In principle, any kind of surrogate function $f_{DEL_{fm}}(z)$ for each considered failure mode fm and for the power production $f_P(z)$ needs to be found to determine the relationship for an arbitrary input $z = (x, u(x))$. The fit is based on short-term DELs computed for a set of input samples of the external conditions and the control setpoints which are denoted as $\hat{z} = (\hat{x}, \hat{u}(x))$. The value $DEL_{fm}^{st}(\hat{z})$ surrogate models can be calculated on the basis of the short term DELs. Thus, the strong non-linearity due to the wöhler exponent does not have

730 to be considered and the damage increments can be calculated using Eq. (19). The short term DEL $DEL_{fm}^{st}(z)$ is obtained
through aero-elastic simulations of the wind turbine model and a subsequent evaluation using the rainflow counting algorithm
and Eq. (16). ~~Also, the mean power is computed $P(\hat{z})$.~~

~~To account for the randomness in the incoming wind and offshore also wave conditions, various realizations of~~ By using
surrogate models to compute damage and energy increment, additional uncertainties are inevitable when calculating long
periods of time. At the same time, the load calculation of wind turbines is always associated with uncertainties due to the
735 ~~same mean input characteristics are usually simulated. Those are determined through pseudo-random seeds. Therefore, the~~
~~total simulation time is the time of a single aero-elastic simulation times the number of seeds. The outputs of the simulation~~
~~are always scaled so that they match the corresponding time span Δt for the damage rate which will be used to compute~~
~~the damage progression. The sampling of \hat{z} needs to be chosen so that it matches with the~~ stochastic influences of the
wind (Mozafari et al., 2023). This must be taken into account when creating surrogate models. Depending on the application
740 ~~and effort, different requirements are made on the surrogate modelling approach. Classical interpolation usually requires~~
~~fullfactorial sampling of \hat{z} so that the number of samples increases exponentially with the dimension of z , i.e. the number~~
~~of input variables, and thus leads to a high number of computationally extensive load simulations. For a low number of inputs,~~
~~however, a fullfactorial sampling allows for a deeper understanding of the results in every combination. It also allows for~~
~~interpolation, which has a major advantage of a straight-forward implementation and no need for tuning of hyperparameters~~
745 ~~of the surrogate model. Due to the randomness in the input conditions, which is reflected to varying degrees in the behavior of~~
~~the DELs, interpolation is often not a suitable approach. Additional requirements result from the necessary suitability of the~~
~~surrogate model for the application in optimisation. For gradient-based optimization, differentiability of the surrogate model is~~
~~required or at least a sufficient smoothness for computing the difference quotient. One major input which also influences~~
~~the choice and applicability of the surrogate model is the control setpoints. The surrogate needs to be able to cover the~~
750 ~~influence of the control setpoints on the loads in a deterministic way, despite the stochastic influence of the wind. A specific~~
~~surrogate model for the application examples is selected in Sect. ??.~~ With the surrogate model computing the damage rate,
the optimization problem can be built for the operation planning models. For example, more accurate models are required for
fatigue tracking or for calculating the remaining service life than for use in an optimization. Here, fast evaluation and good
mapping of the correlations between optimization variables and initial values are of particular importance.

755 ~~The surrogate models for optimal planning need to be able to represent the relation of the derating setpoint to load reduction~~
~~for each external input condition adequately. In addition, a deterministic differentiable function is helpful, if not even required,~~
~~to be used for optimization. Due to the high number of optimization variables, gradient-based optimization is favoured over~~
~~heuristic optimization approaches, which makes differentiability a requirement for convergence criteria. Within this work, the~~
~~main purpose of the surrogates model is to use it as an instrument for showing the long-term optimal planning approach and~~
760 ~~not finding a perfectly suiting surrogate for this purpose yet. Finding a surrogate for any intermediate data point also means,~~
~~that any intermediate value of percentage power between $\delta_P = [50\%, 100\%]$ can be selected. Using the approach, which is~~
~~presented in ??, a continuous selection of derating would be theoretically possible by providing the according setpoints in~~
~~partial and full-load. If a continuous derating or a discrete selection of control methods is advantageous or feasible for a~~

765 real-world application will depend on the use specific wind turbine controller and use case. In order to model the relationship between percentage power reduction and induced damage for optimization, a continuous surrogate model is advantageous and the discrete selection of a setpoint can be implemented on the operating stage.

~~Multidimensional surrogate is considered as an existing prerequisite with various suitable approaches from the literature ranging from gaussian regression (often referred to as Kriging), polynomial chaos expansion to artificial neural networks (Dimitrov, 2019; Hübler, 2019; Slot et al., 2020; Gasparis et al., 2020; Debusscher et al., 2022; Singh et al., 2022).~~

770 A good overview of different surrogate methods and a comparison of their performance is given in Dimitrov et al. (2018). Despite their known lower accuracy compared to some of the other methods, we select multidimensional polynomial regression models ~~are selected as surrogate models~~ for the DELs due to their suitability for optimization, their simple usage, their differentiability and their fast training and evaluation time. For the electrical power, a linear interpolation is used. ~~Replacing the selected methods by other models which were described in Sect. ?? will not affect their application for this purpose if suitability for optimization and accuracy is sufficiently tested.~~

775 To obtain the parameters of the polynomial regression model for the DELs, a least squares approach

$$\min_q \|f_{DEL_k}(\hat{z}; q) - DEL^{st}(\hat{z}),\|$$

is used. The vector q denotes the coefficients of the polynomial, where the maximum degree of 5 is found through the validation error from a cross-validation process. ~~In this case, $DEL^{st}(\hat{z})$ are the results obtained from aero-elastic load simulations within the system boundaries defined in Sect. 3.1. 6-10-minute simulations with 6 different pseudo-random seeds of the wind fields are performed, and the outputs are obtained at the time scale $\Delta t = 1 h$. A fullfactorial sampling for the local input conditions The pool of input conditions is created with a fullfactorial sampling for the wind conditions x together with the percentage power is defined, i.e. together with the percentage power $u(x) = \delta_P(x)$. The sampling values are provided in Table 2.~~

785 The sampling values are provided in Table 2. While wind speed and power are sampled equidistantly, the sampling of the TI values is selected so that the distance between the samples increases exponentially, as indicated by the formula in Table 2. This reduces simulation time and still creates enough data, in situations with high occurrence. To account for the randomness in the incoming wind various realizations of the same mean input characteristics are usually simulated. Those are determined through pseudo-random seeds. For the simulations performed in this work, 6 simulations of 10 minutes on the seconds scope are performed to obtain a damage increment in the minutes scope with the time increment $\Delta t = 60min = 1h$ as it is standard for DEL-calculations.

Table 2. Input sampling for load simulations

Wind Speed \hat{v}	Turbulence intensity \widehat{TI}	Percentage power $\hat{\delta}_P$
4,5,...,25 m/s	$(\sqrt{2})^i \% \forall i = 2, \dots, 11$	$(\sqrt{2})^i \% \forall i = 2, \dots, 11$
		50,60,..., 100 %

790 To obtain the parameters of the polynomial regression model for the DELs, a least squares approach is used. The ~~short-term DELs are obtained using the rainflow counting algorithm as described in Sect. 2.2 for the selected failure modes (See Sect. ??).~~

For the further usage, i.e. the computation of the damage rates being used for optimization, the surrogate models $DEL_k^{st}(x, u(x)) = f_{DEL_k}(x, u(x))$ are used and transferred to a damage rate by Eq. (19). The linear interpolation of power $P(x, u(x)) = f_P(x, u(x))$ is directly used as mean value over the time span Δt .

Within this section, two things are presented and discussed. On the one hand, the accuracy maximum order of the polynomial is set to 5. The value is found by cross validating different orders of the polynomial between 1 and 8. For the further usage of the surrogate fit on the data needs to be evaluated. On the other hand models, it is important to understand the relationship between external input condition, control setpoint and DELs, to be able to assess the selected control methods and also to interpret the long-term planning results. The first point can be examined by looking at the overall error between simulated data and the surrogate model first, but also by a detailed assessment of the surrogate for certain input combinations. The latter can also be used, to address the second point, i.e. for an interpretation of the simulated behaviour.

Removed figure

Previous figure 5 is removed

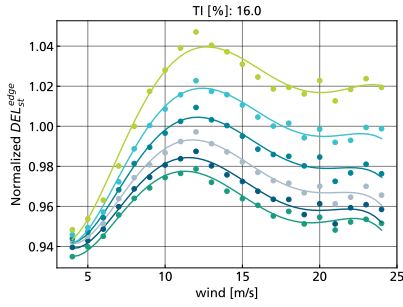
At first, the output of the surrogate model is plotted against the simulated data in particularly important that the influence of the derating setpoint at the different input condition is correctly represented. For all three failure modes, a general agreement of the surrogate model to the data can be observed. Fig. ?? and the relative absolute error on the data (training error) is computed. Afterwards, one of three inputs is fixed and 7 and Fig. 8 exemplary show the evaluated surrogate model (solid lines) as well as the simulated training data (dots in same colour as solid line) are shown exemplary for the other two inputs in Fig. 7 and Fig. 8. For all three failure modes, a general agreement of the surrogate model to the data can be observed in all of the figures. For when one of the input conditions is set to a fixed value. The DELs are normalized with respect to the fixed values ($v = 8m/s$ and $TI = 16\%$) at the nominal percentage power $\delta_P = 100\%$. The power is not explicitly shown here, because its behaviour dependent on wind speed directly derives from the control setpoints (cf. Fig 6c). In general, the accuracy of the fit for the flapwise bm and the tower bm, the error is significantly higher than for base bm is lower than that of the edgewise bm (see figure titles). This can also be observed by the higher spread of the data points for these two failure modes in Fig. ?? and the higher deviation of datapoints to the surrogate fit in the other plots. This is mainly caused from the higher dependency on the wind turbulence, which also creates more variance in the. These loads are more strongly influenced by the turbulence of the wind and thus also have a higher uncertainty in the simulated DELs. Especially for the tower, the high variation in the simulation data makes it difficult to create a surrogate model. One can see from Fig. 7 and Fig. 8 that the models performs well in some regions but worse in others. The error could be reduced by creating a higher number of simulations for training, either with more samples or with more random seeds. In addition, a different approach for the surrogate models like gaussian regression or neural networks as mentioned in Sect. ?? could be applied. Overall, the models fit sufficiently well for demonstrating the optimal planning approach, while further improvements are certainly possible and also required for a more accurate result. Also, the relative mean error on the complete dataset is highest for the tower bm (error=3.88%), compared to the error in flapwise bm (2.32%) and the edgewise bm (0.23%).

825 Error in training data for polynomial regression surrogate models

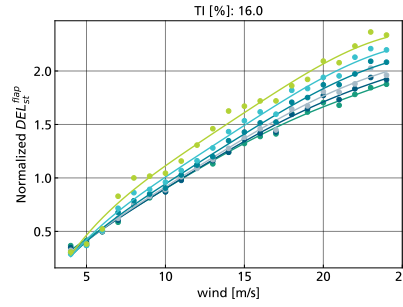
The reason for the low accuracy of the surrogate model on the DELs of the tower bm is also caused by the varying influence of the control setpoints on the DELs. By taking a closer look on Fig. 7 and Fig. 8, such details about the behaviour of the DELs can be seen. The behaviour of the DELs depending on the control setpoints will now be briefly discussed. Figure 7 shows the results with the wind speed v on the x-axis for different values of percentage power $\delta_P = 100\%$ with a fix $TI = 11.3\%$. All values are scaled by the output $v = 11 \text{ m/s}$, $TI = 11.3\%$ and $\delta_P = 100\%$ so that the relative behaviour of the DEL and the power can be seen. The most important part is, to evaluate the influence of the derating setpoint at different input conditions. The electrical power reduces as expected for all wind speeds. $TI = 16\%$. Both, the flapwise and the tower DELs (DEL_{flap}^{st} and DEL_{tower}^{st}) strongly increase with the wind speed (cf. Fig. 7b and Fig. 7c), while the DELs of the edgewise bm DEL_{edge}^{st} reduce when the rated wind speed is reached at 12 m/s and the turbine starts pitching. The load reduction of the edgewise bm directly corresponds to the reduction in rotor speed, and thus (cf. Fig. 7b). The reduction in DEL_{edge}^{st} depending on $\delta_P = 100\%$ directly relates to the lower rotational speed through the control setpoints at each wind speed. Thus, it has a stronger effect at 90 % and 80 % when the rotor speed is lowered by a higher amount than the generator torque to achieve the power setpoint. The decrease of DEL_{edge}^{st} is also rather small compared to the other two failure modes, where the relative difference in DELs is much higher. The DEL_{flap}^{st} can be reduced for almost all wind speeds. In the partial and the full load region, the load reducing effect is higher at larger values of δ_P (80 and 90 %) due to the dependency on the rotational speed (cf. Fig. 7b), but not by the same amount. The DELs of the tower bm show a much less clear relation to the percentage of power. For low wind speeds, the DEL_{tower}^{st} also decrease with the derating lower values of $\delta_P = 100\%$, but with some significant variation within the simulated data points. For higher wind speeds, reducing the power can even increase the tower loads, and the relation is not completely deterministic. As mentioned in Sect. ??, this This effect is caused by the reduced aero-dynamic damping due to the rotor speed reduction or from resonance effects. Implementing active damping for the tower or using different control configurations could reduce this effect. It also shows the conflicting behaviour of the different failure modes.

Figure 8 shows the result with the results with TI on the x-axis for different values of δ_P with a fix wind speed $v = 8 \%$. The power and the DEL_{edge}^{st} are not significantly influenced by the turbulence. The load reduction of the edgewise DEL is low compared to the other two failure modes. For the flapwise bending moment and the tower bending moment, the strongest relative reduction can be achieved by reducing the power to 90%, but more derating still decreases the DELs slightly further. The relative load reduction also increases with increasing turbulence.

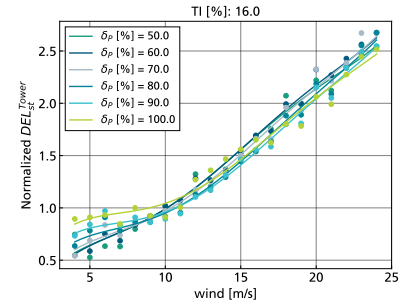
The results presented in this section show several aspects which are relevant for the optimal planning approach. On the one hand, it is possible to determine the relationship between those inputs with a single deterministic function in a simplified way. Advancements in surrogate modelling, control design and damage modelling can be used to create even more suitable models without changing the overall process described within this paper. On the other hand, the results also show the difficulties which arise from the random turbulent inflow and the conflicts between different failure modes for load reduction. A continuous reduction in power does not necessarily result in a continuous reduction of loads and the high nonlinearity between the inputs, the aero-elastic model and the controller can not fully be covered by a simple regression model. Because the essential part of the nonlinearity is covered, however, the The selected method for derating is suitable to reduce the short term DELs and



(a) normalized short-term DEL of edgewise bm

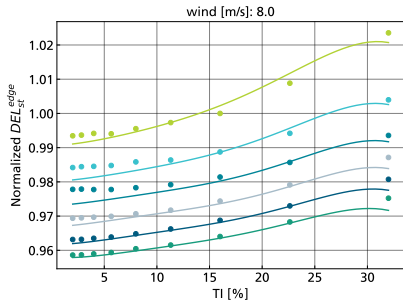


(b) normalized short-term DEL of flapwise bm

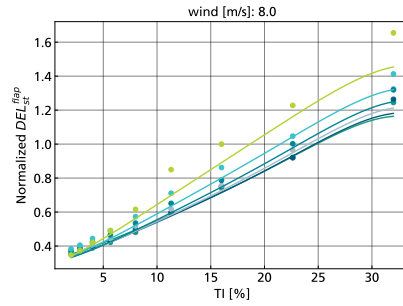


(c) normalized short-term DEL of tower bm

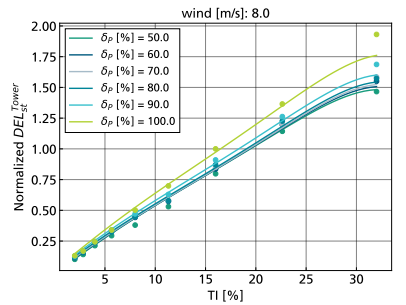
Figure 7. Evaluated surrogate models (solid curves) and simulated data points (dots) for a fix TI of 16% normalized with the short term DEL of the nominal strategy $\delta_P = 100\%$ at $v=8\text{m/s}$ and $\text{TI}=16\%$



(a) normalized short-term DEL of edgewise bm



(b) normalized short-term DEL of flapwise bm



(c) normalized short-term DEL of tower bm

Figure 8. Evaluated surrogate models (solid curves) and simulated data points (dots) for a fix wind speed of 8 m/s normalized with the short term DEL of the nominal strategy $\delta_P = 100\%$ at $v=8\text{m/s}$ and $\text{TI}=16\%$

~

Comment on figure

Colors of figures 7 and 8 are updated

860 [thus the damage increments of all the failure modes. Also, the surrogate models are able to cover the nonlinearity sufficiently](#)
[to be used for further optimization.](#) The optimal planning approach can make use of this to determine when a load reduction
 should be favoured over a higher energy production. This can especially be done by exploiting the fact that higher turbulence
 significantly increases loads, but the power production remains almost the same. This effect is even strongly enforced from
 the relation of the short-term DEL to the damage [rate-increment](#) because the value is raised to higher power by the Wöhler-
 865 exponent (see Eq. (19)). ~~When, and by how much derating is beneficial to apply, can be determined by including the overall~~
~~frequency distribution of each situation in the long-term planning approach.~~

Evaluated surrogate models (solid curves) and simulated data points (dots) for a fix TI of 11.3%. Evaluated surrogate models (solid curves) and simulated data points (dots) for a fix wind speed of 8 m/s.

3.4 Step 3: Determine optimal condition-based operational strategies for lifetime planning

870 4 Method for optimal long-term planning: VIOLA (Value Integrated Optimization of Lifetime Asset operation)

Comment to reviewers

This section contains content of several previous sections and now summarizes the operational planning process comprising of steps 3 and 4.

- Section 4.1 combines the content of previous Sections 2.4 and 4.3. The previous application example was also modified, The former example of section 4.1.2 "Levelled farm damage" is removed
- Section 4.2 combines the content of previous Sections 2.5 and 4.4.

875 ~~The central part of this work is to build up the optimization problem which allows creating an optimal planning of the damage progression over a long period of time or the entire lifetime respectively~~ Having created the surrogate models depending on the selected control setpoints as prerequisites, they can now be used to determine how much derating is beneficial to apply, through the optimal operational planning method. The process for the assessment of lifetime objectives dependent on the operational strategy is shown in Fig. 9. The lifetime objectives are modelled by making use of the surrogate approach on the annual scope. The total damage determines the lifetime of the wind turbine, which influences total energy production and total value. While the total energy and damage define the objectives on a technical level, maximizing the total value is the final goal. All of them are influenced by the setpoints for the operational strategy which determine the optimization variables. The key of the method
880 is to formulate the problem in such way, that a control setpoint is found for each external condition while these long-term objectives are fulfilled. We refer to value as a general measure for the overall valuation of the considered wind energy system. It will usually contain an economic valuation, but my also include other factors such as environmental impact or contributions to grid stability. We call the framework for this method VIOLA (Value integrated optimization of lifetime asset operation). The process shown in Fig. 9 forms the basis for the formulation of the optimization problem which currently consists of the two
885 separate steps, namely steps 3 and 4 of the complete process (cf. Fig. 2).

4.1 Condition-based optimization of operational planning (Step 3)

Building up the mathematical optimization process for finding the operational strategies is the central part of this work. Neglecting economic factors and other ~~restrictions~~ influences and restrictions for the total value of a farm at first, it is ecologically most beneficial to get the maximum amount of energy over the lifetime τ_{life} of the turbine while the fatigue budget of
890 each component is fully used up. ~~Within this work, we set a single turbine and its surrounding external influencing conditions~~

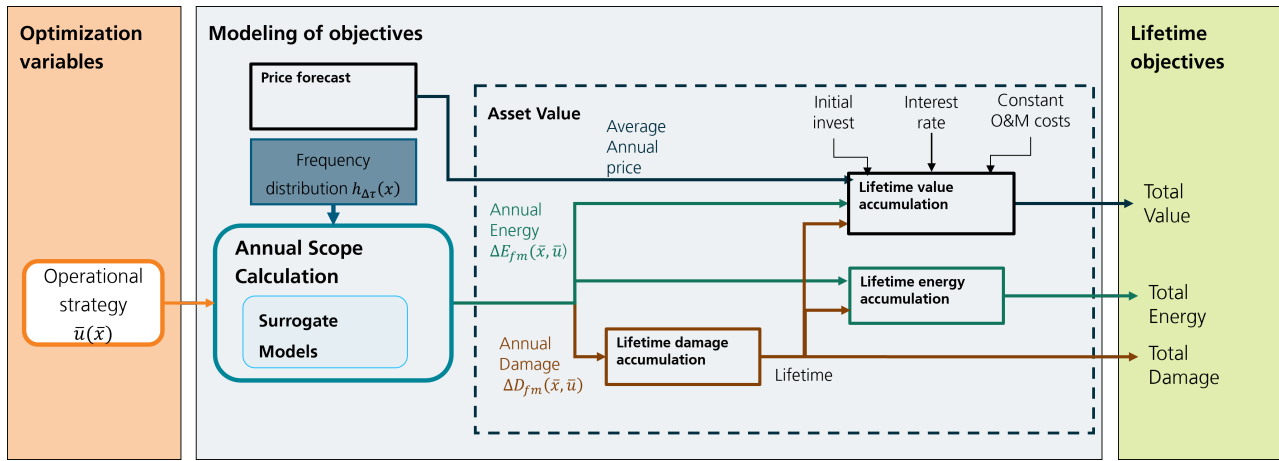


Figure 9. Process for computing the lifetime objectives dependent on operational strategy. The setpoints of the operational strategy define the optimization variables. They are input the annual scope calculation based on surrogate models and frequency distribution. With the output of this calculation, annual damage and annual energy can be accumulated to a lifetime value. The lifetime is determined from the total damage and thus and input for lifetime energy and lifetime value accumulation. The lifetime value is computed with additional inputs for the specified value metric.

Comment on figure

Figure 9 is new to clarify the modelling of the lifetime optimization problem

as the system boundary and the mathematical formulation of this problem is presented in a general form. More details on the system boundaries of the application example are provided in Sect. 3.1.

Therefore, the total energy for a given target damage budget is maximized over the fixed reference time τ^{ref} . The operational strategy $\bar{u} = \{u(x_j)\}_{j=1}^{B^x}$ is optimized for each of the external conditions which were previously selected by the definition of the system boundaries. It follows, that the number of selected independent control setpoints, defined by $Dim(U)$ and the number of bins which are used for the external conditions B^x , determine the number of optimization ~~variables~~ variables, which is equal to $B^x \cdot Dim(U)$. Within the scope of this work $Dim(U)$ is equal to 1 because a single derating strategy will be applied. With a fixed known target fatigue budget D_{fm}^{target} for failure mode $fm \in \mathcal{F}$, the optimization problem is formulated as

$$\begin{aligned}
 & \max_{\bar{u}} \sum_{j=1}^{B^x} P(x_j, u(x_j)) h^{ref}(x_j) \\
 & \text{subset to } \sum_{j=1}^{B^x} d_{fm}(x_j, u(x_j)) h^{ref}(x_j) \leq D_{fm}^{target}, \forall fm \in \mathcal{F}.
 \end{aligned} \tag{22}$$

Using this simple and compact formulation, it is possible to spare the fatigue budget when the damage ~~rate-increment~~ is high compared to ~~power-production~~the energy increment. When the damage of all failure ~~modes~~ is reduced compared to a baseline operation \bar{u}^{ref} , i.e. $D_{fm}^{target} \leq D_{fm}^{ref}$, the turbine can be operated for a longer time and ultimately more energy can be produced.

905 The optimization problem is solved by using the gradient-based interior point algorithm for constrained non-linear optimization problems (Wächter and Laird, 2022). The process itself is formulated with Python and the optimizer is interfaced through the library pygmo (Biscani and Izzo, 2020a) which builds on the C++ library pagmo (Biscani and Izzo, 2020b). Gradients are computed using finite differences. Optimization runs were executed on a laptop with Intel i7 four-core processor, 2.1 GHz speed and 32 GB RAM. The execution time of each run ranges from several minutes to several hours, depending on the specified target damages. The optimizer typically needs between 100 and 500 iterations to converge. As starting values, the reference strategy
910 with 100% power production at each turbine was always used, which is a non-optimal but feasible solution. All optimization runs show plausible results in terms of an improved relationship between energy increment and damage increment. For this reason, no explicit variations of the starting values were required to check for convergence to local minimal.

Clearly, the solution strongly depends on the selected failure modes, their behaviour of the damage rate determined from the surrogate models and on the target fatigue budget. When several failure modes should be optimized simultaneously, it might be
915 impossible to fulfill the constraints and no solution can be found. Therefore, the selection of the target budget strongly depends on the specific problem which is individual for a specific wind farm or wind turbine respectively. ~~On the one hand, many other factors need to be considered in order to decide when and how a component should be allowed to fail, depending on the relevant failure modes. A major factor are component costs, which will determine if a failure leads to a decommissioning of the turbine or a simple exchange, which needs to be aligned with maintenance planning. On the other hand, the formulation in~~
920 The formulation in Eq. (22) provides a clear separation of the technical aspect from the economic aspect, and therefore allows investigating the relationship between damage progression and energy production for different components under consideration of the operational strategies over long periods of time. The formulation of (22) It can also directly be used to create the a Pareto-front between damage and energy production by principally applying the Epsilon-constraint method for multi-objective optimization (Chiandussi et al., 2012), i.e. by fixing various combinations of the target values D_{fm}^{target} . This approach is applied
925 ~~in Sect. 4.1.1. Some economic aspects which arise from a financing model for debt repayment are covered in the fourth step, which is applied in Sect. ???. The underlying financing model is explained in the next section. We pursue this approach within this work, and select a specific strategy based on further in formation in the final step 4.~~

4.2 Step 4: Select economically best operational lifetime-planning strategy

5 Application of four-step method

930 ~~With the specified system boundaries, the four-step procedure described in Sect. 1.3 can be applied to the demonstration example. At first, the specific choice for the derating method is explained. Afterwards, the results of the load surrogate models are presented, mainly to understand the influence of the control setpoints under the input conditions. Afterwards, the optimization problem is conducted for two different use cases pursuing different goals. At first, levelling the damage of all~~

turbines of the artificial wind farm is intended. Secondly, the trade-off between annual damage and energy production is found separately for each of the selected failure modes in the form of Pareto-fronts.

4.1 Step 1: Provide adaptable real-time controller of the wind turbine

4.1 Step 2: Build surrogate models for damage progression and energy production

4.2 Step 3: Determine optimal condition-based operational strategies for lifetime planning

4.1.1 Creating Pareto-optimal solutions for the application example

The general problem, which was formulated in Sect. ??, is applied on two different use cases for the example wind farm. At first, the damages of two failure modes are levelled within the example wind farm. As a second step, a Pareto-front is created for each failure mode separately. The results of the Pareto-front are subsequently selected based on an the economic model in Sect. ??.

The optimization problem is solved by using the gradient-based interior point algorithm for constrained non-linear optimization problem (Waechter and Laird, 2022). The problem itself is formulated with Python and the optimizer is interfaced through the library pygmo (Biscani and Izzo, 2020a) which builds on the C++ library pagmo (Biscani and Izzo, 2020b). Gradients are computed by using finite differences.

4.1.2 Levelled wind farm damage

Before applying the optimization problem, the example wind farm with 9 turbines is investigated with the reference operational strategy \bar{u}^{ref} where all turbines operate at $\bar{\delta}_P = 100\%$ both in partial and in full load operation. The total energy production and the total damages of the considered failure modes are evaluated using Eq. (??) and Eq. (??). The energy production and damages are computed under the assumption that the We apply the optimization method to the considered turbine in the centre determines the design conditions, i.e. the reference of the wind farm. To do so, we first need to define the reference design value DEL^{ref} . It is computed with the combined wind probability distribution of that turbine including the wake effects . Principally, it means that site-specific wind distribution, including wake effects for wind and TI and with the reference operational strategy \bar{u}^{ref} is already adjusted to the specific site. This is clearly not the approach, which is usually applied for design load calculations, but it is advantageous to understand the relative differences between the turbines caused from the wake-induced turbulence. Due to the low assumption for the ambient turbulence, computing DEL^{ref} with the IEC wind class 1A results in significantly lower damage values of all turbines for the tower and the flapwise bm. To show the benefits of the condition based-optimal planning, the current reference is beneficial, however. Therefore, the total damage of that the considered turbine is equal to 1 for all failure modes in accordance with the introducing explanation in Sect. 2. Consequently, the total damage of each turbine is always relative to the turbine in the centre with all turbines operating at 100 % because of the relationship determined from Eq. (19). The resulting damages with all turbines operating with the reference operational strategy $\bar{\delta}_P = 100\%$ in all situations is referred to as the reference case.

965 The results for this case are shown in Fig. ???. While the differences in energy production and the damage of the edgewise
 bm lie around 2-4% only (see Fig. ?? and Fig. ??), there is a strong variation of damage on the tower and the blades in flapwise
 direction (see Fig. ?? and Fig. ??). The high relative differences of more than 0.5 for the flapwise bm and more than 0.3
 for the tower bm are mainly due to the wake-induced turbulence. Such high differences consequently mean, that the turbine
 with lowest induced damage could be operated much longer than the weakest turbine when only looking at fatigue damage
 970 for instance. Without considering adaptive strategies for the long-term planning, this currently means that all turbines will be
 over-designed so that the weakest turbine is able to withstand the induced loads.

Damage and energy production in the example wind farm relative to the turbine in the centre (turbine no. 4). Through a
 levelling of fatigue damage of all turbines, a longer operation of a complete wind farm would be possible without any changes
 on the structure. For both, the tower and the flapwise bm, the turbine in the lower left corner has the lowest total damage at
 975 about 0.70 of the turbine in the middle. Therefore, the target values for the optimization problem defined in (22) are defined
 as $D_{flap}^{target} = D_{tower}^{target} = 0.7$ for each of the 9 turbines except for the lower-left one. The damage of the edgewise bm is not
 considered in this case, resulting in the following formulation for the optimization problem:-

$$\begin{aligned} & \max_{\tilde{u}_s} \sum_{j=1}^{B^v} \sum_{i=1}^{B^{TI}} P(v_j, TI_i, u_s(v_j, TI_i)) \tilde{h}_s^{ref} \\ \text{subset to } & \sum_{j=1}^{B^v} \sum_{i=1}^{B^{TI}} d_{tower}(v_j, TI_i, u_s(v_j, TI_i)) \tilde{h}_s^{ref} \leq 0.7 \\ & \sum_{j=1}^{B^v} \sum_{i=1}^{B^{TI}} d_{flap}(v_j, TI_i, u_s(v_j, TI_i)) \tilde{h}_s^{ref} \leq 0.7 \end{aligned}$$

980 The results of solving the problem defined in (??) for each of the $s = \{1, \dots, 9\}$ turbines separately are shown in table ??.
 The total damages with respect to the reference case are computed for all of the selected failure modes. For all 9 turbines,
 the damage can be reduced to the value of 0.7 as specified by the constraints. While the optimization is performed using
 a probability distribution for the local wind speed and turbulence (from Eq. (??)), the total damage is computed with the
 distribution for wind speed and wind direction (from Eq. (??)). This causes slight deviations so that the damage sometimes
 985 aggregates to a value slightly higher than 0.7, e.g. for turbine number 8. This deviation definitely lies within the margin of
 overall uncertainty.

The strong benefits of the approach can be seen when looking at the relative results for each turbine compared to the
 reference case, as shown in table ??. While the damage of the flapwise bm and of the tower bottom can be reduced at maximum
 to about 0.54 and 0.70 respectively, there is a much smaller loss in energy production to about 0.93 at maximum. For each
 990 turbine, the relative damage reduction of the flapwise bm and the tower bm is higher than the relative energy. Since the loss
 in energy only refers to the same time span of τ^{ref} , it would be more than compensated through the extended lifetime from

the damage reduction. The lifetime extension factor for a single failure mode is the reciprocal of the relative damage value according to Eq. (9). By levelling the total damage of all turbines in the farm through operational strategies, an alignment of decommissioning or maintenance of the turbines also becomes a major advantage. One also has to state that the damage of the edgewise bm between the different turbines is not aligned anymore. This is due to the strong difference in influence from wind speed and turbulence intensity on the different loads. Therefore, it is clear that the influence of control on the different failure modes must be carefully balanced and will always depend on the constraints from a specific turbine and site as well as on the specified system boundaries.

Result of optimization for each turbine (total damage and energy production with reference from turbine 4 (in the centre))

Result of optimization for each turbine (relative damage and energy production compared to operation without derating)

To get a better understanding This is a strong assumption that will not hold true in reality for different reasons. However, it allows a simpler interpretation of the results in detail, we exemplarily select the turbine in the center, i.e. turbine number 4. It is the turbine with highest damage on the tower and affected by the wake of turbines from all directions. The distribution of annual wind frequency, energy production and damage with standard operation are shown in Fig. ?? and Fig.12. In each plot, the wind speed is plotted radially and the wind direction circumferentially. The relative annual frequency at the site is given in percent, i.e. by $100 \cdot p_{\Delta T}^{ref}(v^{amb}, \theta^{amb})$. The damage and energy production are given by their total value share on the overall value during τ^{life} , i.e. by

$$\frac{d_{fm}(f_4^{wake}(v^{amb}, \theta^{amb}), u^{ref}) h^{ref}}$$

$$\frac{P(f_4^{wake}(v^{amb}, \theta^{amb}), u^{ref})) h^{ref}}$$

and respectively.

The highest frequency in the wind distribution occurs in south-western direction (Fig. 5c). This distribution is also strongly reflected in the energy production (Fig. ??) and the damage of the edgewise bm (Fig. ??). Contrary to this, the highest amount of damage for the blades in flapwise direction and the tower is induced in wind direction downstream of surrounding turbines from all directions.

The results of the optimized strategy are shown in Fig. ?? . For the plots, the results depending on local wind speed and turbulence are transferred back to values depending on ambient wind speed and wind direction by sorting the results into corresponding bins. While optimization based on local wind speed and direction reduces the number of optimization variables, an implementation of the strategy based on wind direction is easier to apply in reality in an open-loop setting of the planning approach. Figure ?? shows the optimization variable, i.e. the percentage of power for each input condition. One can clearly see that derating is mainly applied when the turbine is in the wake of the neighboring turbines. The highest derating of 50% is applied in the combinations of low wind speeds and high turbulence intensities because this is most beneficial for the tower loads. When comparing the optimized damage rose for the flapwise bm (??) and the tower bm (??) to the standard operation, one can clearly see the reduction of damage in the regions with a high damage contribution. Especially when the wind comes from the north or the south, the neighboring turbines are in close distance to the selected turbine and thus damage can strongly

be reduced. This optimized derating strategy exploits the fact that reducing damage under those conditions is highly beneficial because a high amount of damage is induced while the energy production is comparably low.

As mentioned before, the derating of each turbine also influences its own wake, which consequently influences the neighboring turbines. Therefore, the process for levelling the damage of all turbines is not completely fulfilled, and wake effects would need to be recomputed with the new optimized planning strategy or the problem would need to be solved for all turbines at once. It also depends on the selected control setpoints and selected failure modes if the effect of derating on the damage of the turbine itself is higher than the indirect effect through wake reduction on neighbouring turbines. Especially for the tower, this can be highly beneficial following some of the studies mentioned in Sect. ?? like Bossanyi and Jorge (2016) or Meng et al. (2020). Overall, this approach requires an expansion of the system boundaries to a system of interacting systems.

While levelling the damage between all turbines within a specified time period is one use case, another can be determined when looking more closely on a single turbine. Due to the specification of damage reduction, the extended lifetime is actually fixed through the deterministic relationship at this point. We limit ourselves to the factors that can be influenced beyond design decisions and safety factors. Therefore, each reduction of damage of a failure mode results in an extended lifetime according to the deterministic assumption from Eq. (10). Thus, it is actually neglected as an important degree of freedom. By finding the Pareto front of energy production and damage, the desired lifetime can be selected on the basis of those results. The selected turbine in the centre is also used for this second use case.

Distribution of frequency and energy production for all wind directions (plotted circumferentially in degrees) and wind speeds (plotted radially in m/s) for the center turbine of the example wind farm

Original distribution of damage (without applying derating) for all wind directions (plotted circumferentially in degrees) and wind speeds (plotted radially in m/s) for the center turbine of the example wind farm

Optimized derating strategy and associated distribution of damage for all wind directions (plotted circumferentially in degrees) and wind speeds (plotted radially in m/s) for the center turbine of the example wind farm

4.1.2 Pareto front for energy and damage

As it was mentioned in Sect. ??, the Epsilon-constraint method can be directly applied on the optimization problem defined in (22) to find a Pareto front. By solving the problem for various values of $D_{fm}^{target} \in [0, 1]$, the maximum amount of energy for each of these values can be found. For simplification, each failure mode is considered separately. On the one hand, this increases the interpretability of the results. On the other hand, it would be applicable if the weakest failure mode of a turbine or component can clearly be determined.

For each failure mode $fm \in \{flap, edge, tower\}$, at first the minimum possible damage is computed as an orientation. Then
 1055 the optimization problem

$$\begin{aligned} & \max_{\tilde{u}} \sum_{j=1}^{B^v} \sum_{i=1}^{B^{TI}} P(v_j, TI_i, u(v_j, TI_i)) \tilde{h}_4^{ref}(v_j, TI_i) \\ \text{subset to } & \sum_{j=1}^{B^v} \sum_{i=1}^{B^{TI}} d_{fm}(v_j, TI_i, u(v_j, TI_i)) \tilde{h}_4^{ref}(v_j, TI_i) \leq D_{fm}^{target}. \end{aligned} \quad (23)$$

is solved with $D_{fm}^{target} \in \{0.65, 0.7, \dots, 1\}$ for the $fm \in \{tower, edge\}$. For the flapwise bm, the damage can be reduced down
 to a minimum of 0.24, so that the values $\{0.25, 0.3, 0.4, 0.5, 0.6\}$ are added to the previous set to define the values of D_{flap}^{target} .
 1060 Therefore, several optimal planning strategies are computed constraint between 0.3 and 1 depending on the failure mode
 to obtain desired points the three Pareto-fronts. Each point yields an optimal planning strategy separately for each failure
 mode denoted as \tilde{u}_{fm}^{opt} . Such a strategy is denoted as \tilde{u}_{fm}^{opt} .

The results of the optimization for each failure mode, i.e. the Pareto-fronts, are shown in Fig. 10 where the relative energy
 production percentage energy production compared to the reference case is plotted over the relative damage total damage
 1065 which is equal to 1 for the reference case. When comparing the results, one can clearly see the different behaviour of the failure
 modes, which results from the determined relation of the damage rates to the control setpoints and the external conditions.
 While it is possible to significantly decrease the damage of the flapwise bm (Fig. 10c) and the tower bm (Fig. 10b) without
 losing much energy, the edgewise damage can only be reduced with comparable losses in the energy production. This is mainly
 due to the fact, that the dependency of the edgewise bm on TI is low lower and that damage can mainly be reduced by reducing
 1070 the rotational speed, as it was partially discussed in ???. The strong relation of energy production and induced damage of the
 edgewise bm can also well be seen be comparing Fig. ??? and Fig. ???. Therefore, the applied method has a much bigger potential
 for turbulence induced loads, as it was already expected from the behavior for each of the DELs, as presented in Sect. ???.

As mentioned earlier, reducing Reducing the damage results in a factor for lifetime extension which is approximately deter-
 mined by Eq. (9) under the limitations discussed in Sect. 2. According to Eq. (11), the energy yield after the extended lifetime
 1075 $\tau_{fm}^{life}(\tilde{u}_{fm}^{opt}) - \tau_{fm}^{life}(\tilde{u}_{fm}^{ref})$ is also increased by that factor. Additionally, the selected failure mode is assumed to be the only one
 relevant to life extension so that the damage of the others can be neglected for this example. By directly maximizing the energy
 production, the maximum amount of energy can be produced while fully using up the fatigue budget of the failure mode with a
 variable time span in this case. The result of this optimization is shown as an orange dot a large blue dot in Fig. 10 and Fig. 11.
 Figure 11 additionally shows the relative energy production for each failure mode plotted over the relative damage.

1080 For the edgewise bm, only a slight increase of the energy production of about 25% can be obtained when the damage is
 reduced between 0.85 and 0.9. From below 0.75, the damage reduction even results in a loss of energy and is thus not effective
 anymore. 0.75 and 0.85. For the tower bm and the flapwise bm, the amount of damage reduction is always stronger than the
 loss in energy so that the, the reduction of damage leads to a lower loss in energy than for the edgewise bm. Therefore, the
 overall energy production after the extended lifetime can be significantly increased. For the tower, reducing the damage down
 1085 to 0.68 results in the highest energy gain of 35% by up to 17% when damage is reduced down to 0.77. A further damage

reduction reduces the effect ~~slightly~~significantly. The strongest positive effect can be seen on the flapwise bm due to the combined influence of the selected control method, the strong influence of high wind speeds and turbulence, as well as the high Wöhler-exponent. The damage can be reduced down to a value of 0.25 resulting in an increase of energy by more than factor 3. While the additional energy production for the tower bm almost increases linear at first and then reaches the maximum value at ~~0.7~~0.77, it clearly shows a more than linear growth for the flapwise bm. ~~However, the loss of energy and thus the extension factor have a similar value for both, the flapwise and the tower bm. When the damage is reduced down to 0.7.~~

~~Overall, the results show that effectively reducing the damage has a large potential to increase the energy production from a given budget. This especially holds true for certain failure modes where derating is more effective under high loading external conditions. The computed Pareto-fronts represent a trade-off between damage and energy production over a given time period. Selecting which trade-off is the best can additionally be assessed by an economic evaluation, which is conducted in the following section.~~ between damage and energy production over a given time period, of which a single value and corresponding strategy need to be selected to complete the 4-step process. Before we apply this step, the resulting operational strategies for each result which yields the highest relationship between energy and damage are investigated more closely (large blue dot).

4.1.2 Detailed results of a single optimization run

To be able to interpret the optimized operational strategies, the distributions of damage with reference operation are shown for each failure mode in Fig. 12. In each plot, the wind speed is plotted radially and the wind direction circumferentially. The damage values are given by their total value share on the overall value during τ^{life} .

The highest frequency in the wind distribution occurs in south-western direction (see Fig. 5c). This distribution is also strongly reflected the damage of the edgewise bm (Fig. 12a) and partially of the flapwise bm (Fig. 12b). While the highest amount of damage is induced at wind speeds below rated for the edgewise bm, the flapwise damage distribution is dominated by the high share at high wind speeds in south western direction. For both, the flapwise bm and also the tower bm (Fig. 12c), there is high share of damage when they are subject to wake from the upstream surrounding turbines. The resulting operational strategies, which are optimized to reduce each of the failure modes while maximizing energy production, are shown in Fig. 13. The results depending on local wind speed and turbulence are transferred back to values depending on ambient wind speed and wind direction by sorting the results into corresponding bins. While optimization based on local wind speed and direction reduces the number of optimization variables, an implementation of the strategy based on wind direction is easier to apply in reality in an open-loop setting of the planning approach. In all three operational strategies, the reaction to the high damage in the situations, where the turbine is in the wake of other turbines, is visible. In such situations, the damage is increased due to the wake-induced turbulence while energy production is decreased due to reduced wind speeds. This leads to a high benefit of reducing power in such situations. In addition, each of the strategies reflects the individual behaviour of the selected failure modes and of the influence by the control setpoints under the specific conditions. While slight reduction in power, especially at low wind speeds, maximizes the energy production with the constraint on the edgewise bm (Fig. 13a), the strategy with the flapwise constraint mainly reduces power at high wind speeds (Fig. 13b). With the tower bm constraint, the selects the lowest possible setpoint of 50% at low wind speeds up to 8 m/s in addition to the slight reduction in waked situations (Fig. 13c).

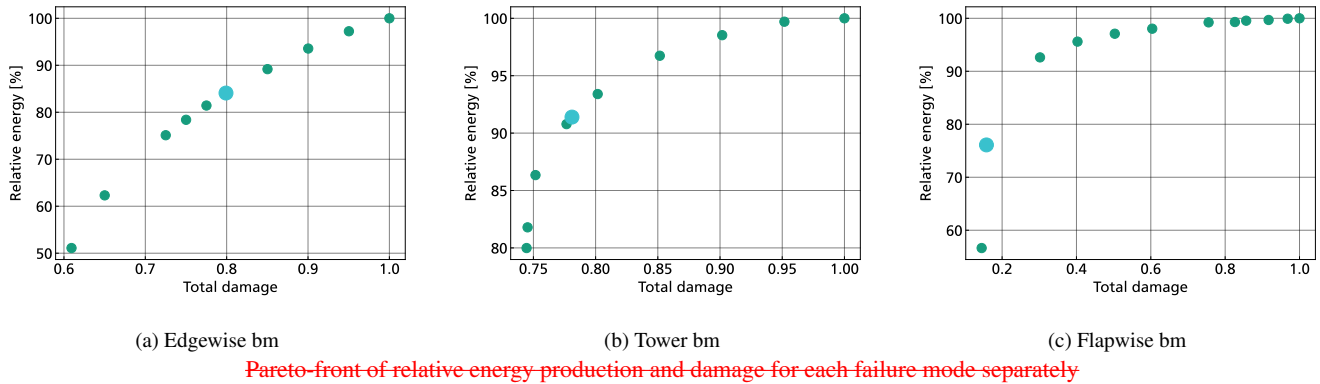


Figure 10. Pareto-front of relative energy production and damage for each failure mode separately

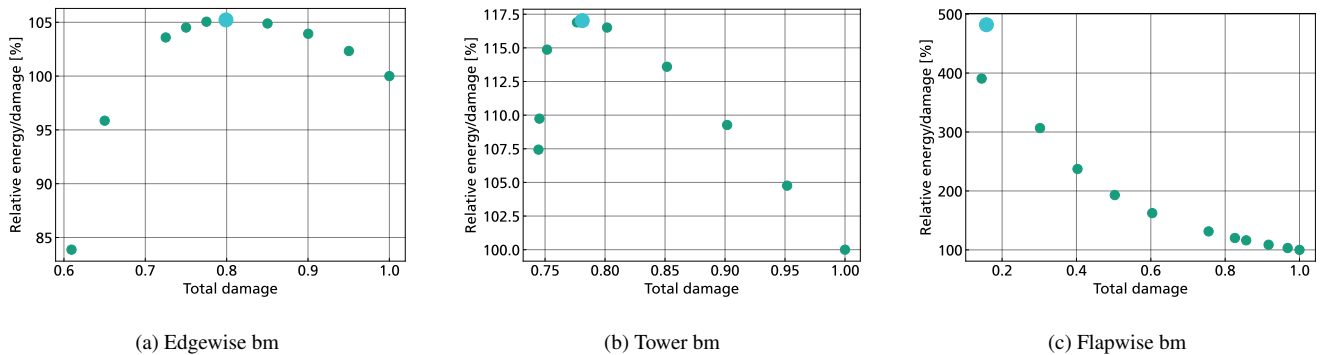


Figure 11. Relative energy over damage plotted over the relative damage for each failure mode separately

Comment on figure

Colors of figures 10 and 11 are updated. The results are also updated due to changes of the ambient TI input the input for the model.

1120 Due to the selected method of the real-time controller, a significant load reduction can mainly be achieved at such low wind speeds for the tower. The strategies thus result overall from the interaction of the selected method and setpoints of the real-time controller, the derived surrogate models and the specified objectives of the optimizer.

4.2 Selection of best solution (Step 4: Select economically best operational lifetime-planning strategy)

1125 With the presented optimal planning approach, higher total energy yield can **only** be achieved with lifetime extension, which **in turn is only is** made possible by accepting lower **yearly annual** energy production throughout the lifetime. **With the approach presented in Sect. ??, more energy can be obtained from the utilized materials, but the economic impact is neglected.**

A first evaluation of the effect of optimized operational planning on total revenue is possible with a simplified approach that includes a This reduction of annual energy has a significant impact on the overall value of the wind farm, especially when

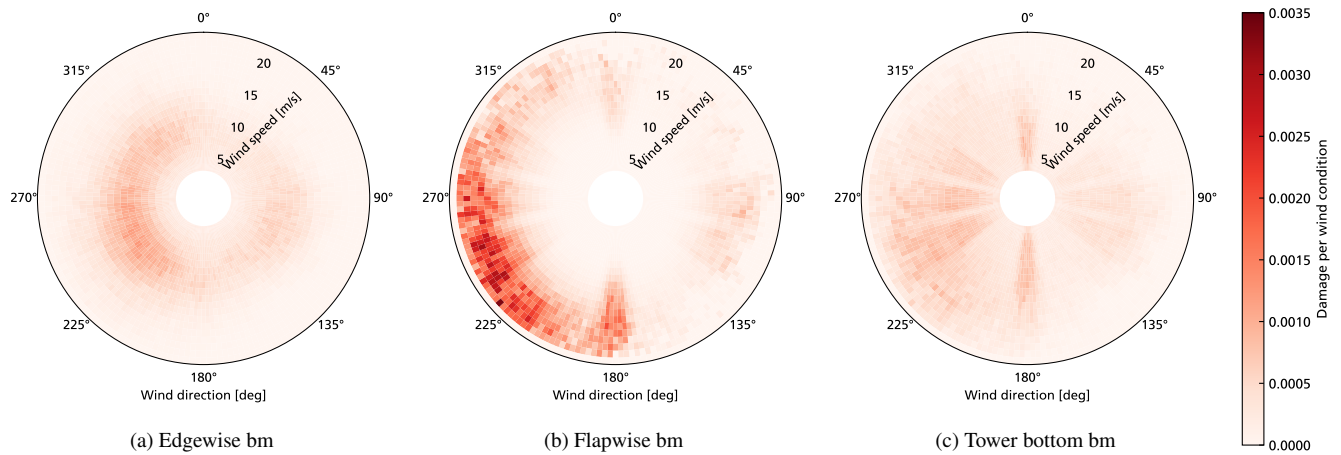


Figure 12. Relative energy over Original distribution of damage (without applying derating) for all wind speeds (plotted over radially in m/s) and all wind directions (plotted circumferentially in degrees) of the relative-considered turbine in the centre of the wind farm

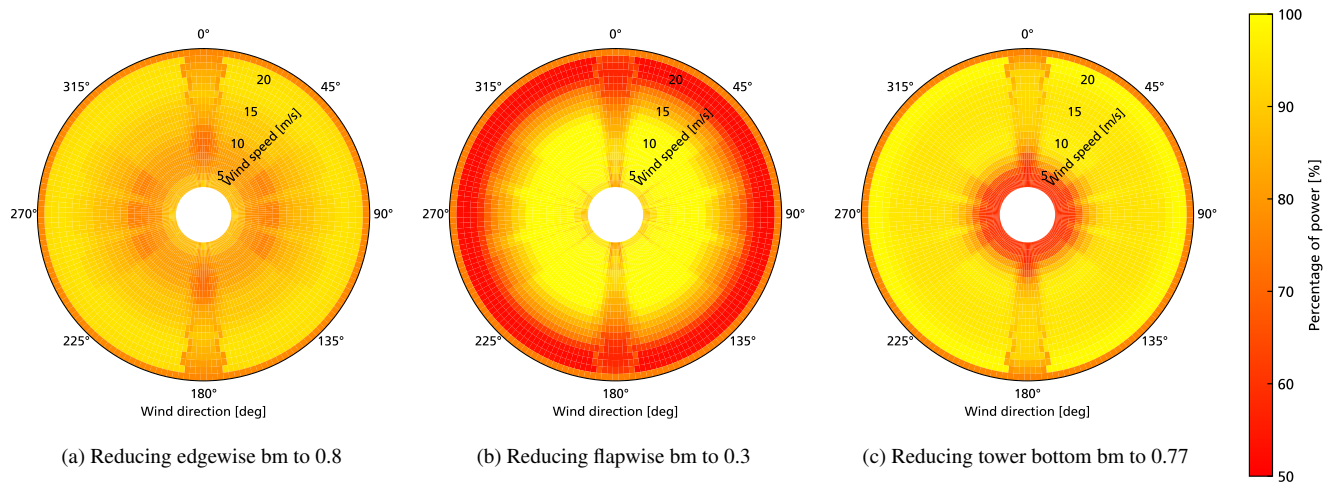


Figure 13. Selection of optimized operational strategies. Each of them maximizes the total relation of energy over damage for each-one of the failure mode-separately modes. The power percentage values are plotted for all wind speeds (radially in m/s) and directions (circumferentially in degrees)

Comment on figure

Figures 12 and 13 are new figures created with new results.

1130 taking into account economic factors that include loan repayments and the value of money. This aspect is considered by for the evaluation and selection of the operational strategies under consideration of a basic financing model. This is based on the

Through this first evaluation, the difference between a pure maximization of energy from the materials used and additional factors can be emphasized. We use the net present value for this.

4.2.1 Computation of net present value

1135 The net present value NPV ~~,-which~~ maps a future payment to its current value. We assume a constant interest rate C_{WACC} covered by the weighted average costs of capital (WACC), constant annual maintenance costs C_{OPEX} and a constant average price of electricity $C_{elPrice}$. The repayment can be variable over the entire operating period and is made depending on the annual energy yield $E(\Delta\tau; \bar{u}, h_{\Delta\tau})$. Currently, it is assumed to be constant in each year, because we use the same operational strategy and frequency distribution. With these parameters, the NPV can be computed for payments until a given year Y :

$$NPV(Y) = \sum_{t=0}^Y \frac{C_{elPrice} \cdot E(\Delta\tau; \bar{u}, h_{\Delta\tau}) - C_{OPEX}}{(1 + C_{WACC})^t}, \quad (24)$$

1140 The future value at the end of the lifetime of an adapted operating strategy is given by $NPV(Y^{life})$ where the number of full operating years with the strategy is defined as

$$Y^{life} := \left\lfloor \frac{\tau_{fm}^{life}(\bar{u})}{\Delta\tau} \right\rfloor. \quad (25)$$

This model maps all future payments to their current value, and thus also gives an upper bound to the initial investment that is permissible. Any revenue above the initial investment leads to additional profit.

1145 ~~In Sect. 4.1.1, each of the three failure modes were already considered separately. An economic evaluation is most important for tower damage. A tower replacement is usually considered to be infeasible, which in turn determines the possible lifetime of the entire wind turbine. An exchange of the rotor blade, in contrast to this, can be a feasible approach to extend the turbine's lifetime when one of its failure modes has reached its fatigue budget. Having this in mind, it is still advantageous to create a planning for these replaceable components in order to coordinate the replacement of several blades or to find the best timing. Considering all of these aspects would require further detailed models on component costs and the specific situation of a wind farm. A second reason, why the tower damage is most suitable for the economic evaluation, can be derived from the previous results. Due to high damage reduction of the flapwise bending moment, very long lifetime extensions would be possible. In contrast, the edgewise bending moment only offers a small potential for a beneficial lifetime extension. The major drawback for the consideration of the tower loads is the fact, that the influence of the selected derating method on the tower loads is subject~~

1155 ~~to the highest uncertainty among the three failure modes and can sometimes even have negative impact, as it can be seen from the results in Sect. ???. Despite that, the optimal planning results from Sect. ??? show that it is still possible to significantly reduce the damage when it is applied under suitable conditions. Reducing the uncertainties would be required for an adaption to a real turbine.~~

1160 ~~In order to select a trade-off based on the economic benefits, the net present value from Sect. ??? is used. The~~ The average costs for a wind farm are taken from BVG Associates (2019); they are summarized in Table 3. All values are scaled to a single turbine with 7.5MW power. ~~The numbers are actually valid for a full~~ financial estimations refer to an entire wind farm, so that

scaling it to a single turbine is not fully realistic. It can ~~rather be seen as an examination of the entire wind farm~~ be interpreted as the "per turbine" costs of a farm. Therefore, all of these values are very rough assumptions which just allow for the possibility to compute the potential increase in profit within a realistic range.

Table 3. Overview of parameters for financing model

CAPEX per MW	OPEX	Change rate	WACC
2.37 Mio £/MW \approx 2.73 Mio. €/MW	76 k£/MW \approx 87.4€/MW	1.15 €/£.	6 %

1165 The annual income is computed with the reference annual frequency distribution and the operational strategies from the results. An availability factor of 0.95 is assumed. In addition, we assume an electricity price of ~~0.066~~0.064 €/kWh at which the wind farm is barely able to recover the investment cost after a lifetime of 25 years, when being operated with the reference strategy \bar{u}^{ref} .

4.2.2 Selection of strategy based on net present value

1170 In Sect. 4.1.1, each of the three failure modes were already considered separately. We first make a preselection of the strategy by limiting ourselves to a single failure mode. An economic evaluation is most important for tower damage. A tower replacement is usually considered to be infeasible, which in turn determines the possible lifetime of the entire wind turbine. An exchange of the rotor blade, in contrast to this, can be a feasible approach to extend the turbine's lifetime when one of its failure modes has reached its fatigue budget. Having this in mind, it is still advantageous to create a planning for these replaceable components in order to coordinate the replacement of several blades or to find the best timing. Considering all of these aspects would require further detailed models on component costs and the specific situation of a wind farm.

1175

The financing model using the NPV from Eq. (24) is applied to all of the derating strategies which were computed for the tower in Sect. 4.1.1. The lifetime of the turbine is always determined as the time after which the induced damage has reached the fatigue budget, i.e., by Eq. (10). For the final year, the annual income is computed as a fractional value, depending on relative damage increment before the value of 1 is reached. Here, the seasonal variations discussed in Sect. 2 are neglected.

1180

The results are shown in Fig. 14. In all three subfigures, the green dashed curves correspond to the Pareto-optimal points from Fig. 10b. The ~~orange-blue~~ curves highlight the one trade-off, where the maximum energy is being produced over the extended lifetime, which is almost ~~37-32~~ years. The ~~red-light blue~~ curves highlight the operational strategy with best economic results, i.e. the highest NPV at the lifetime where the damage equals 1. It results in a relative damage value of ~~0.8-0.9~~ and an extended lifetime of ~~slightly more than 31~~about 27 years. Since the same frequency distribution for wind conditions and the same operating strategy is assumed for each year, also the annual damage and annual energy production are equal. This results in a linear increase of the damage in Fig. 14a and the energy production in Fig. 14b. Fig. 14c shows the net present value representing the permissible investment if the system was operated until a certain year.

1185

The assumed initial costs (CAPEX) are equal to about $7.5 MW \cdot 2.73 \text{ €/MW} \approx 20.4 M\text{€}$. It can be seen ~~clearly~~ that

1190 for maximum energy generation, the system ~~has to be operated at least 35 years until it is economically viable, whereas the~~

reference strategy and the economically optimal strategy require only about 25 or 26 years of operation respectively. At 35 years, the NPV of the strategy which maximizes energy is nevertheless about 0.25 M€ higher than the value with the reference strategy at 25 years. The difference of the reference strategy and the economically optimal strategy require about 25 or 26 years of operation respectively to exceed the CAPEX. The strategy which maximizes NPV is achieved with a target damage of 0.9 at a lifetime of 27 years. The difference to the reference strategy at 25 years is about 1.39 M€. Also, the strategies with target damages of 0.95 and 0.9 reach a higher NPV compared to the reference strategy.

Therefore, both optimized these strategies will pay off after a longer operating time, but the strategy maximizing NPV leads to a significantly higher NPV at an earlier time. This can also clearly be seen from Fig. 14c. The under the given circumstances. In contrast to this, the reduced energy yield per year of the strategy maximizing total energy (orange curve bright blue curve with dots) leads to lower income, lower repayment per year and in turn to lower NPV over the entire lifetime compared to the strategy which maximizes NPV (red curve dark blue curve with crosses) and the reference strategy (dark green dashed curve).

For all strategies, it must be noted that the assumed WACC of 6% needs to be taken into account as well. While the net present value does not change significantly in later years, the profit would increase strongly once the investment has been repaid. Thus, the actual profit can be multiplied with $(1,06)^r$ where r is the number of years operating once the investment has been returned. Therefore, a slightly higher NPV can already result in much higher profits.

Overall, the assessment of economic benefits always needs to be done under consideration of the specific assumptions and parameters for a specific project and can be done in much more detail. Especially the price of electricity underlies a high uncertainty and can hardly be predicted for 30 years in the future. Nevertheless, the exemplary evaluation shows how multiple optimized planning strategies can be used to obtain an economically optimized solution, depending on the objectives and input parameters.

5 Discussion

With the application example, we aimed at showing that all four identified steps build on one another and how the process can be used for an effective distribution of damage over the entire lifetime of a turbine. This way the interaction of the inputs The application of all four steps to the application example has shown the interaction of inputs (e.g., control setpoints), such as control setpoints, environmental conditions, damage progression and energy production, becomes clear. Step 1 establishes the connection from selected setpoints on supervisory control level to the effect these have on the real-time controller. The transfer of the setpoints to parameters of the real-time controller results in changed loads and power production. This leads to a change in the behavior of the damage rates depending on the external conditions, which is expressed by the surrogate models created in step 2. Therefore, the selection of a control setpoint determines how effective the damage can be reduced for a single input condition at a time scale of $\Delta t = 1h$. energy production and economic value. The distribution of the damage progression follows for the long-term perspective by determining the optimal strategies in step 3. This step was conducted for two different use cases. The first use case, where the damage of all turbines within the farm was reduced to the same

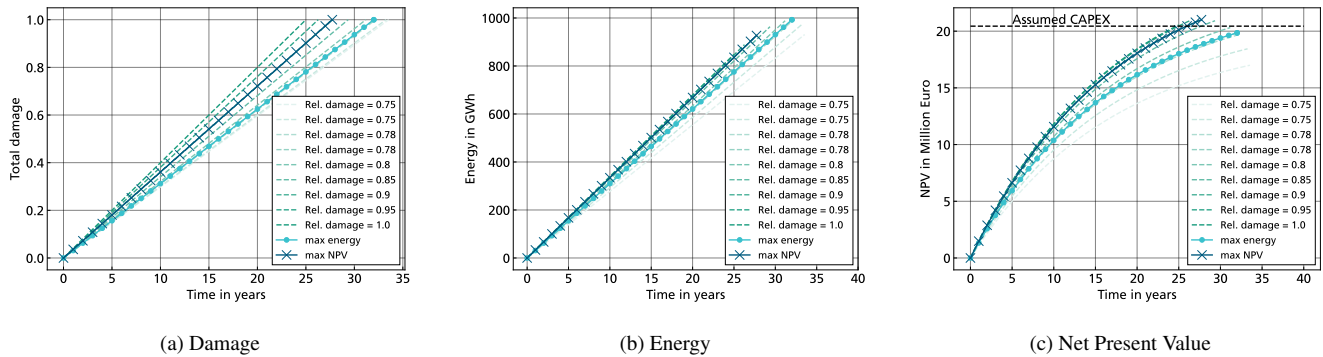


Figure 14. Annual progression over time for accumulated damage, energy, and profit NPV for multiple optimized planning strategies (Green: results of Pareto-front; Orange-Bright blue with dots: Maximum energy production; Red-Dark blue with dotscrosses: Maximum profit NPV)

Comment on figure

Color of figure 14 is updated. The results are also updated due to changes of the ambient TI input the input for the model.

level, is not followed by the fourth step because the technical objective is, for the time being, independent of the economic evaluation. The main purpose of this use case was to show the technical benefits of the optimization approach. For the second use case, where multiple planning strategies are optimized for a single failure mode of one turbine, adding the fourth step allows for an economic evaluation of the strategies at first and subsequently helps to select the best overall trade-off considered example mainly illustrates that the mathematical optimization method is applicable for creating operational strategies and how the method can be used to exploit the full load-bearing capacity of one component and to increase the value of the considered system. The mathematical optimization builds on the assumptions of the underlying models and their input data. It finds the best operational strategy under these assumptions in a deterministic way. The resulting deterministic lifetime extension factor includes these assumptions, and should therefore be interpreted as a potential value that needs to be validated by further assessments.

The solution also includes the uncertainties resulting either from model inaccuracies or from uncertain assumptions in the input data. This inherent limitation must always be taken into account when evaluating and discussing the results. For this reason, we have taken great care to describe the required prerequisites in detail. In addition, we have limited ourselves to the technical level first when performing the optimization (step 3). The consideration of economic factors is subject to a high degree of uncertainty due to the uncertainty of future electricity prices and other influences which are not considered. The selection of an operational strategy must always be made for a specific application, taking into account the inherent uncertainties and risk. The selection process applied in this work mainly aims at showing how the economic aspect can be taken into account and that an intelligent operational strategy can lead to higher economic profit when selected carefully.

~~Within the specified system boundaries,~~ The presented method VIOLA yields a deterministic optimal solution, which is intended as operational plan for an uncertain future. Therefore, on the one hand, it has to be discussed how the uncertainties

of the deterministic solution can be reduced by improved partial models. On the other hand, current limitations of the method and possible extensions have to be named.

5.1 Limitations and possible improvements on partial models of the current approach

The optimization process builds on the usage of surrogate models. They implement the deterministic relationship from inputs to damage and energy increments on the minutes scope. Within these models, the advantages of the approach become evident in both use cases. As a result of the condition-based optimization, limits and uncertainties of various partial effects are aggregated. This includes the modeling of input conditions, the high fidelity simulation model on the seconds scope, the induced damage is saved exactly where the relation to the energy production is unprofitable. This can explicitly be observed on the results of a single turbine, as shown in Fig. ???. While the turbine is operated with its reference control at $\delta_P = 100\%$ most of the time, it is not worth inducing a high amount of damage when the energy production is comparably low. This is mainly done when the turbine operates in the wake of another turbine. Principally, the result could be interpreted as a sector management plan. In contrast to simple sector management schemes, the planning is provided in such way, that the amount of damage reduction for each inflow condition is just sufficient to meet the overall damage target while energy production is maximized calculation of damage increments and finally the selection and training of the surrogate models themselves. The modeling approach for each of these is very closely linked to the specified system boundaries.

In each of the optimizations carried out, either for levelling the overall farm damage or to create a Pareto-front of multiple results, the individual optimal distribution for the specified objective and constraints is found. The importance of a suitable specification of these becomes apparent with the second use case because multiple trade-offs between damage and energy production can be found for each failure mode. This use case also shows that it is not only possible to gain more energy from the given fatigue budget, but also to create a significantly higher profit. Both, the increase of energy and profit, result from lifetime extension due to overall damage reduction as it can be visibly observed in Fig. 14b. For the application example, we have limited ourselves to two main environmental conditions and one controller setpoint as considered input conditions. These inputs define a subset and can be extended for both, environmental conditions and the possible setpoints. Fatigue damage of structural components is represented by three main failure modes. Discussing the complexity of fatigue damage modelling goes beyond the scope of this paper; instead, readers are referred to e.g., Liao et al. (2022), which provides an overview about developments in this field.

Through the introduction and the description of the theoretical background of the individual steps, it has also become clear that the results are generally subject to some assumptions and that some influencing factors are neglected. Furthermore, the results of the example always depend on the defined system boundaries, which additionally do not take some influences into account. In principle, therefore, a distinction must be made between limitations and potential improvements of the approach itself and limitations for the specific application example.

The approach relies on the use of surrogate models, which have a limited validity and implement a deterministic relationship from inputs to damage rates. Therefore, the results are only valid for the utilized model. The use of various surrogate models for the computation of site-specific damage has extensively been discussed in Sect. ???. Without the use of surrogates which

explicitly include the influence of the turbine controller, only a single operational strategy can be employed. The selection of a single reference operating strategy for the turbine also relies on assumptions about future wind conditions and damage progression, e.g., specified by standard IEC design wind classes. Thus, by involving adaptive control as an instrument, a site-specific operation of a turbine under specified targets becomes possible, and surrogate models are suitable for its optimization. In the end, the uncertainties of Regarding the environmental conditions, further influences like wind shear, yaw misalignment, wave effects for offshore wind farms can be considered. In addition, the wake-effects of surrounding wind turbines can be modelled with a higher level of details to cover effects like partial wake overlap or wake meandering. This requires an extension of the models on the minutes as well as the seconds scope.

The control setpoints of the surrogate model for the adaptive planning need to be estimated together with other design and operating assumptions. Those need to be considered for the specification of suitable safety margins, together with real-time controller act as inputs to the surrogate model and as influencing variables for the optimizer. Thus, by extending the number of controller features which can be adapted and used as optimization variables, the possibilities for balancing damage under various environmental conditions increase. It would be ideal to directly optimize the control parameters under all influencing load conditions and select the trade-off according to the overall objectives, including their frequency of occurrence. Such an approach is not computationally feasible due to the need for load simulations under each condition in combination with a control parameter. Therefore, extending the possibilities of re-adapting the planning based on the long-term performance evaluation of the turbine, changed long-term targets or improved surrogate models.

Besides this general dependency of the approach on the surrogate model, there are some limitations in each of the four steps, which influence the results. When the setpoints for the real-time controller are provided in step one, the degrees of controller combined with a smart pre-selection of further control setpoints, such as allowing for partial overload or wake steering, will lead to more degrees of freedom for the optimization is limited by the choice of a single setpoint. On the one hand, the applied derating strategy can be fine-tuned to create a higher load reduction on the tower, for example. Also, a power-boost could be included as a percentage factor. On the other hand, adding additional control setpoints increases the possibilities of planning the damage progression, but also the number of inputs for the surrogate model and in turn the number of optimization variables. long-term operational planning. With limited computational capacities, a balance between accuracy, degrees of freedom, interpretability of results and also enhancement of the approach needs to be found for specific use cases and for the optimization process itself. To assess the importance of various influences on the results, sensitivity analysis could be performed, but this is beyond the scope of this paper.

The choice of input conditions is part of the specification of system boundaries and has an influence on the results of the use case. Within the application example,

5.2 Long-term forecasting models and uncertainties

While partial models could theoretically be improved until they provide a perfect representation of reality, the forecasting over long periods of time will always be subject to remaining uncertainties. Therefore, prediction of the future always contains assumptions, which are usually modelled by a probabilistic approach. For the long-term forecast, one can distinguish between

1315 ~~the technical part, where the forecast of environmental conditions influences the fatigue damage calculation, and the system boundaries have been defined quite narrowly to explicitly demonstrate the approach for wake induced damage increases. Adding further external input conditions is explicitly covered by the general approach. This is mainly done in step 2, because each input requires an extension of the surrogate model for this degree of freedom and the underlying simulation model needs to be able to cover the effects of those inputs. Covering the wake effects through wake induced turbulence is a strong simplification which neglects the dynamics of the wake and partial wake effects forecasting of the economic developments. This is affected by many unknowns from the global market and even politics.~~

1320 ~~Regarding the technical part, we use the classical approach for the computation of fatigue damage by covering the long-forecast by a relative frequency distribution derived from site-specific measurements from the past. In combination with partial safety factors, such an approach is suitable for estimating a conservative design fatigue budget. Nevertheless, they neglect some important influences like annual variations of the wind (Pryor et al., 2018). Also, wind shear and yaw-misalignment as well as grid events and idling could also be included. For offshore wind turbines, including a model of the ground, the foundation in combination with wave influence would be required because reducing the aero-dynamic damping through control can have an even higher negative influence than it was observed in the present example. Overall, the determination of the relevant input conditions for the system boundaries must always be considered in conjunction with the possible setpoints for the real-time controller, since it is this coupling that is ultimately exploited for optimized planning.~~

1330 ~~In addition to the consideration of external inputs in the surrogate models, including them within the statistical frequency distribution of the condition is also required. Here, one long-term changes in the weather due to climate change could become relevant. Hübler and Rolfes (2021) found a low influence on fatigue life compared to other influences, but pointed out their potential influence with improved methods. For a more detailed estimation for each individual turbine, probabilistic approaches for the fatigue damage prediction using surrogate models can be used, e.g., by using monte-carlo simulations with a representative time series (Hübler, 2019) or by using stochastic distributions for modelling the uncertainty (Nielsen et al., 2021). Due to the high computational effort, such approaches are less suitable to be used within an optimization loop. The probabilistic approach for fatigue life prediction is strongly connected with the choice of inputs for the models. One also needs to distinguish between conditions which are influenceable by the can be influenced by control setpoints of the controller during power production, such as the additional wind influences mentioned above, and conditions that cannot be influenced (e.g., idling), but which nevertheless participate in contribute to the overall damage process. For the application example, including a frequency distribution of the ambient turbulence would increase the accuracy of the results, as a first step. For the choice of inputs, one needs to balance between accuracy, computational cost and relevance of each input for the damage progression and the setpoints of the real-time controller. Therefore, it is also possible to reduce uncertainties with further details in the models. To determine the overall risk, it is required to assess the uncertainties of the partial models and the forecasts.~~

1345 ~~Furthermore, setting the system boundary at a single turbine is a limitation that has already been mentioned. Solving the optimization problem for each turbine individually neglects the influence of the turbine controller on the wake and thus on the surrounding turbines. To include this effect, the system boundary needs to be extended to a complete wind farm and the optimization problem would need to be formulated for all turbines at once. Then, the control setpoint of the upstream turbine~~

influences the local input conditions and thus the damage progression of the downstream turbine. This way, it would also be possible to combine derating with wake steering for damage reduction and power maximization. However, this approach has the drawback that the number of optimization variables increases. At first, the local frequency distribution created in Sect. ?? cannot be used anymore to decrease the number of optimization variables by binning the wind conditions into wind speed and TI because the wind directions need to be considered within the optimization problem. Additionally, the number of variables is proportional to the number of turbines. Overall, solving the problem for a complete wind farm including the interactions through control for all input conditions at once is a feasible approach, when sufficient computational power for the increased number of optimization variables and input conditions is available. Using an iterative approach where the resulting planned operational strategies for each turbine is fed back to the wake modelling program would be possible.

Within step 3, i.e. the determination of the condition-based strategy through mathematical optimization, the formulation of the target damage as constraints is In our current implementation of the proposed method, a limitation of the approach because it requires a preselection of the target damage values. This might not always lead to optimal or even feasible solutions. Specifying the target values for an increasing number of failure modes resulting from wider system boundaries, e.g. by considering a system of systems like a wind farm, thus requires a high understanding of the system and the pursued targets. Levelling the damage of one or more failure modes of all turbines is still a valid approach, but might not be achievable in all cases. Therefore, selecting a solution based on multiple optimized strategies under consideration of further information like economic factors can overcome this issue. Within this work, multiple strategies constrained by different damage targets were found to create a Pareto front in Sect. 4.1.1. This approach is currently restricted by using a single failure mode. very basic approach for the economical part, i.e., computing the asset value, is implemented. Regulatory and legal framework conditions are excluded from the model, as they can change over time and are strongly dependent on the specific location. Also, our focus is on showing the technical feasibility. Covering all regulatory aspects and expected, planned or coming legislation is a highly specialized but separate task. Nevertheless, the current approach can be supplemented with further inputs to reduce the uncertainties. Also other value metrics like the cost of valued energy (COVE) could be integrated (Loth et al., 2022). A highly significant influence is the price of electricity which is not constant over the entire lifetime.

~~A combination of step~~ To sum up, the amount of detail in the mathematical optimization process has to be a deliberate decision. This decision also depends on other parameters like the available computational power and the optimization method. With the current subdivision into two parts, the technical, deterministic optimization in step 3 ~~and~~, and the subsequent selection based on additional (economic) factors in step 4 ~~might be a potential approach to create an integrated solution which includes finding suitable damage targets for each~~, the mathematical optimization problem can be solved with low computational effort and the deterministic solutions are well understandable and interpretable. Nevertheless, several drawbacks to our approach remain.

5.3 Limitations and potential improvements of the optimization method VIOLA

Without any limitations on computational power and time, the robust optimization approach which directly maximizes the asset value as an objective containing further inputs like reliability models, component replacement costs, forecasts of the market,

etc. including their probabilistic uncertainty would be ideal. To approach such an ideal solution within given boundaries, several smaller steps can be made.

The deterministic optimization method is currently limited to a single turbine. The influence of the turbine controller on the wake and thus on surrounding turbines is neglected. To extend our approach to an entire wind farm two possible solutions exist. The first way is to optimize operation of all turbines once, but this could increase the size of the optimization problem beyond feasibility. The second solution could be to iteratively cycle through computing inflow conditions for an individual turbine from a wind farm flow model, then optimizing operation for each turbine separately for their respective inflow conditions. We expect such an approach to converge after few cycles, while keeping computational requirements at bay and scaling well. Both solutions allow a combination with farm control solutions, such as wake steering.

Overall, any deterministic solution of a single turbine or an entire wind farm requires the specification of an individual target damage for each selected failure modes. ~~This way, component costs could also be considered. However, combining these steps has two major drawbacks. At first, it increases the complexity of optimization problem, and it requires the consideration of time, because one component can fail earlier than another. Then, the possibility of replacement or repair would need to be integrated. Since replacement will lead to a jump in maintenance costs, it makes optimization more difficult. In addition, considering the probabilistic nature of failure would further increase complexity. Resolving the separation of the technical from the economic level can be seen as a second drawback, because it can reduce the interpretability of results. On the other hand, still separating the technical and economic part for a large number of turbines and failure modes would require to create a many-objective Pareto front and does not necessarily increase interpretability. Solving this issue is still part of upcoming research.~~ Here, the specification of a desired target reliability level for the components of each wind turbine could be covered by probabilistic reliability methods. Further research is required to assess how this can be integrated with the current method. It also needs to be investigated how the computation of any value metric can be integrated into the optimization approach, either directly within the mathematical optimization or for a subsequent selection of Pareto-optimal operational strategies.

Within the application example of this work, selecting the trade-off based on a simple repayment model using the net present value in step four only covers a small of the economic aspect. It does not cover any variable costs for maintenance or prices of electricity. With this approach, it is possible to show that a reduction of the energy production in some situations can still pay off through the extended lifetime. Finding an integrated solution for the economic benefits, in combination with the target values for the damage and the component costs, still requires advancements of the approach. A first extension of our current approach is possible, by allowing ~~To cover the forecast of volatile market prices within the deterministic mathematical optimization, the annual frequency distribution of input conditions can be extended with another dimension for price and thus a combined probability for wind and price, similar to the approach in Loepelmann and Fischer (2022). In addition, an annual selection of the trade-off between energy and damage on the Pareto-fronts, which are computed in Sect. 4.1.1, could be integrated into the optimization.~~ This way, it would be possible to allow for a higher damage progression at the beginning to reduce the interest burden and to reduce the damage progression of the turbine later on.

One aspect, which can not be covered by the current planning approach, is considering sequence effects, i.e., dependencies of future damage progression on previous damage. With the use of frequency distributions for long-term effects, linearity of

damage progression is inherently assumed. To consider sequence effects, the current approach can at least be used as an initial planning step, partially covering the linear part of a damage progression process.

5.4 Application of optimized strategies

1420 Regardless of the limitations, the results of the application example show how a condition-based ~~approach for~~ long-term planning ~~can be used to achieve~~ approach can realize a targeted fatigue damage planning progression. It balances the trade-off between induced damage and energy production under the given system boundaries and constraints of the application example optimally.

1425 It is possible to apply the method to a real-world scenario when the system boundaries are well-defined and adapted to the specific use case. In a first step, the provided planning strategy can be used in an open-loop scenario, where the turbine follows the ~~setpoints of the planning. This requires a sufficiently accurate measurement of the input conditions which are used for the planning. The bin width of the optimization could be adapted according to the measurement accuracy. The planned setpoints.~~ The open-loop approach can also be used, to extend the lifetime after the turbine has already been operating for a significant time span. If the approach is applied during the design process, it could be used to save material through a less conservative design ~~. Therefore, the planning approach already brings a high potential even without a closed-loop operation in combination~~ with reliability control. For applying the approach, some mentioned uncertainties would need to be reduced by adapting the specific use case. Also estimating the amount of uncertainties would be required, or to optimize the power curve as part of the real-time controller.

1435 ~~Relating the approach back to the context of~~ In a second step, the approach could be further developed into reliability-adaptive control, ~~the damage contribution in each wind condition can be used as a setpoint for the where measurements of turbine operation are fed back into continuous re-planning, thus forming a~~ closed-loop controller ~~, which is as~~ presented on the right-hand side of Fig. 1 in Sect. 1.2. ~~In this case, the planning would not provide a setpoint for the controller itself, but the control loop on the operating stage would try to stay as close to the provided planning based on the performance evaluation of the wind turbine or wind farm. The evaluation would need to include the health status of the component. In a first step, this could be covered by using the same surrogate models as for the planning, but with the actual wind conditions as an input.~~ Overall, the open-loop approach using the optimized operational planning already creates significant benefits, which can be further increased by using it for a closed-loop operation. The challenges to do so were partially discussed in Sect. 1.1.

~

6 Conclusion and Outlook

1445 We presented a novel approach method for an optimal planning for the operation of wind energy systems over their entire lifetime. This ~~was achieved by introducing~~ comprises a four-step process, of which the key is to formulate a mathematical optimization problem which optimally distributes the available damage budget of a given failure mode over the total turbine lifetime. Within the introduction, the objectives for this work were derived from the context of reliability(-adaptive) control. A

1450 planning, which pursues long-term objectives of operation, was identified as an important ~~prerequisite~~-input. Our process is focused on the planning of the fatigue damage progression of different wind turbine failure modes. As a basis, the theoretical background for the deterministic computation of fatigue damage progression was introduced. The process is applied to an application example for demonstration, which serves as a proof-of concept.

1455 ~~Following this, the four steps to provide an optimal planning were introduced, starting from providing~~ Each of the four steps is introduced providing some general background and subsequently applied to the demonstration example. The process starts by providing setpoints for the real-time controller of a wind turbine (step 1) ~~;~~ and is continued by their usage as an input for the creation of surrogate models for the induced damage (step 2). ~~Subsequently, those surrogates are used to determine optimally planned operational strategies as results of a~~ Those two steps were identified as required prerequisites for the new method VIOLA consisting of steps 3 and 4. In step 3, the mathematical nonlinear optimization problem ~~(step 3).~~ The selection of the results is ~~is~~ built up and solved using the surrogates from step 2. Several Pareto-optimal operational strategies are found as results. Finally, the results are selected based on an economic evaluation ~~as a final step of the approach~~ (step 4). ~~The theoretical background for each of the steps was provided, including literature researches; then, the method was applied to an example for demonstration. Within this work, the process is focused on the planning of the fatigue damage progression of different wind turbine failure modes. The application example serves as a proof-of-concept for the process. It~~ application example shows the high potential ~~of the approach~~ for an effective ~~damage reduction for two different use cases.~~

1465 ~~The optimization approach in step 3 allows to meet the specified targets of the use cases, because the damage budget can be saved or spent depending on operation conditions such that it pays off most in the long-term perspective. This way, it is possible to gain more energy from a given system and thus to reduce cost and ecological impact by a better usage of materials. Overall, the long-term planning brings great advantages in itself and still offers a high potential for further development of the approach.~~

1470 ~~Limitations to the approach~~ planning of damage progression in relation to energy production. By assessing several strategies based on the economic value, the potential, and risk of such strategies become apparent at the same time. Many of the limitations, assumptions and potential improvements were discussed in ~~great detail in~~ Sect. ~~??~~. ~~These also provide starting points for potential improvements. In general, the separation into four steps allows to create intermediate solutions and to interpret each of them. But it also creates some limitations in itself, like the restriction to pre-selected setpoints for the~~ 5. The key is to use partial models within their assumptions and limitations. They must be carefully examined and tested for ~~each actual use case. Improvements, starting from the~~ real-time controller. ~~A higher integration of the steps, e.g., building or improving surrogate models within the optimization process, could be possible, but requires higher computational power and leads to reduced explainability. The current process thus represents an approach which can be used with currently available methods, despite the mentioned drawbacks. It is applicable with reasonable computational power, and each of the steps can be verified individually. Also, the four steps could principally be applied to most existing turbines with minor adjustments. over~~ the damage calculation with surrogates up to long-term predictions, can be made in the respective domain.

1480 The main field for improvement of the four-step method is to allow it to operate within a broader system boundary. Within our future work, we want to focus on further development of the method VIOLA. Here, one can distinguish between further

improvement of the currently-used deterministic mathematical optimization and the use of probabilistic methods. For the deterministic part, a first step would be an extension of the system boundaries for the operational planning of all turbines in a wind farm at once. In addition, operational strategies need to be able to handle volatile market prices and further requirements of future wind energy systems. This could be combined with control setpoints for uprating or power boost and for grid support. With all these aspects, we aim at integrating wind farm flow control considering electricity prices, as shown in Kölle et al. (2022a), with our optimal planning of the damage progression to increase value of wind farms. Since the deterministic approach for fatigue damage progression neglects the stochastic nature of system and component failures, probabilistic approaches to define target reliability values for each wind turbine as a system can be employed. At first, ~~this means that an extension to optimizing for multiple failure modes at once is required. Secondly, optimizing for coupled systems~~ probabilistic approaches can be used for the selection of the best operational strategy by estimating the underlying uncertainty. Subsequently, it needs to be evaluated if and how the uncertainty assessment can be integrated into the optimization process, e.g., ~~wind turbines that interact through wind farm control, must be possible. In addition, a more advanced financing model might reduce uncertainty and thus yield further benefits for operations. Ideally, this could also include fluctuating electricity prices, which we did not yet take into account~~ using robust optimization methods. Stochastic methods can also be applied to integrate the uncertainties of the future market.

To apply the strategy ~~;~~ ~~a coupling of during operation, coupling~~ the planning stage with the operational stage is required. As a first step, ~~an open-loop implementation control~~ can be implemented. To do so, the properties of a specific wind turbine or wind farm need to be identified and coupled with the planning approach. ~~An adaption~~ Regular readjustment of the planning ~~after some time~~, as also indicated in Fig. 1 ~~with the arrow for "Readjust planning"~~, would allow for a simplified ~~"continuous"~~ semi-continuous adaption of the system based on ~~the~~ current system performance.

In such a scenario, it needs to be examined how short-term deviations from the planning, e.g., by reacting on electricity prices or simply on grid requirements, can be tolerated while at the same time following the provided planning sufficiently well. The best time and way to readjust the planning also ~~needs need~~ to be investigated. Connecting the operational planning with additional inputs like maintenance planning would bring further advantageous to the approach. ~~A real-closed-loop~~ Real closed-loop behavior, where the planning provides setpoints for a reliability controller, has an even higher overall potential but also brings further challenges which were discussed in the introduction already (Sect. 1.1).

~~One aspect, which can not be covered by the current planning approach, is considering sequence effects, i.e., dependencies of future damage progression on previous damage. By binning the relevant deterministic conditions and considering their frequency distribution, the linearity of damage progression is always assumed for long-term effects. In this case, the approach can at least be used as an initial planning step, partially covering the linear part of a damage progression process.~~

~~In addition, the probabilistic nature of failure will need to be addressed for further advancements of the approach, e.g., through sufficient safety margins or by adding uncertainties to the optimization. This is not only caused by the probabilistic nature of failure, but also because the uncertainties of wind prediction and electricity prices cannot be eliminated completely.~~

~~In the~~ In the future, the coupled operation of wind turbines or wind farms with power-to-X systems will become highly relevant. This increases the need for adaptive operation because the damage progression of connected systems also needs to

be considered and the question when to operate each system on what level needs to be answered. Therefore, such a coupled operation leads to a further expansion of the system boundaries and brings more complexity on different levels. For hydrogen
1520 production, the damage progression in an electrolyzer needs to be integrated in order to assess their reliability. It is also necessary to include prices for selling hydrogen ~~and thus~~, and thus to serve a second market. ~~As a first step, it needs to be examined in what way a coupled operation of a wind turbine with an electrolyzer could be influenced by different setpoints of the real-time controller and how this can be used to influence the damage progression of both systems.~~

1525 Concluding, the presented work provides an applicable and adaptable method for the long-term planning of wind turbine operation. ~~It still offers possibilities for further improvements on various levels, as well as potential for research and further development in different areas.~~ More research is needed to reduce uncertainty and consider multiple components and failure modes in the ~~approach on the planning level~~ planning. Additionally, the integration with reliability-adaptive control offers further advancements to discover the full benefits for a more sustainable wind farm operation.

List of symbols

fm	Failure mode
\bar{u}^{ref}	reference operational strategy
τ^{ref}	reference lifetime
\bar{u}^{opt}	optimized operational strategy
\bar{u}	arbitrary operational strategy
τ^{life}	free modified lifetime
$\Delta\tau$	time increment for long-term planning, e.g. 1 year
Y	number of time increments
c^{ext}	extension factor
$c_{fm}^{ext}(\bar{u})$	extension factor for failure mode fm depending on operational strategy
$\tau_{fm}^{life}(\bar{u})$	chosen operation period for failure mode fm depending on operational strategy
Δt	time increment for the definition of input condition, e.g. 1 hour
$x \in X$	external input conditions valid for a time of Δt
$\bar{x} = \{x_j\}_{j=1}^{B^x}$	set of input conditions with B^x bins
B^x	number of bins for all input conditions
x_j	input conditions for bin j
$w = Dim(X)$	number of independent wind conditions
$B^{x^{(w)}}$	Number of bins defined for condition $x^{(i)}$
$u(x) \in U$	setpoints for real-time controller depending on x
$\bar{u} = \{u(x_j)\}_{j=1}^{B^x}$	definition for operational strategy as set of setpoints depending on \bar{x}
$p_{\Delta\tau}(x)$	relative frequency distribution of input conditions
$h_\tau(x)$	absolute frequency distribution of input conditions for a time period τ
h^{ref}	reference absolute frequency distribution which is applied for planning of a site
$D_{fm}(\tau^{ref}; \bar{u}, h_\tau)$	function for damage for a failure mode with variable τ depending on the operating strategy and the frequency distribution as parameters
$\Delta D_{fm}(\bar{u}, h_{\Delta\tau})$	damage-increment <u>annual or mean damage</u> for strategy \bar{u} (time increment <u>period</u> $\Delta\tau$)
$d_{fm}(x, u)$	damage rate-increment for failure mode fm (time increment Δt)
$P(x, u)$	power-production <u>energy increment</u> under the input conditions (time increment Δt)
$E(\tau; \bar{u}, h_\tau)$	function for energy production with variable τ depending on the operating strategy and the frequency distribution as parameters
$\Delta E(\bar{u}, h_{\Delta\tau})$	damage-increment <u>annual or mean energy</u> for strategy \bar{u} (time increment <u>period</u> $\Delta\tau$)
n_i	Number of load cycles
N_i	Maximum bearable number of load cycles

D^{ult}	ultimate design load
m	Wöhler coefficient
L_{ij}	Oscillation amplitude of a load cycle
N^{eq}	Number of equivalent load cycles
$DEL^{st}(x, u)$	short term damage equivalent load
$DEL(\tau, \bar{u})$	lifetime damage equivalent load
DEL^{ref}	reference damage equivalent load
$z = (x, u(x))$	input to surrogate model as combination of external conditions and control setpoints
$\hat{z} = (\hat{x}, \hat{u}(x))$	input sampling for the creation of surrogate models
$f_{DEL}(z)$	surrogate function for DEL of failure mode fm
$f_P(z)$	surrogate function for power production
D_{fm}^{target}	target fatigue budget for failure mode fm
$NPV(Y)$	Net Present Value depending on year Y
$C_{elPrice}$	constant electricity price
C_{OPEX}	constant annual costs for operation and maintenance
c_{WACC}	constant interest rate defined as weighted average costs of capital (WACC)
v^{amb}	ambient wind speed
v	local wind speed
TI	local turbulence intensity
θ^{amb}	ambient wind direction
s	turbine index in a wind farm
S	number of turbines in a wind farm
$f_s^{wake}(v, \theta)$	wake calculation function for a turbine s
$B^{v^{amb}}$	number of bins for ambient wind speed
$B^{\theta^{amb}}$	number of bins for ambient wind direction
B^v	number of bins for local wind speed
B^{TI}	number of bins for local turbulence intensity
M	generator torque
k	generator torque coefficient
M_r	rated generator torque
ω_r	rated generator speed
δ_P	percentage power factor
β	pitch angle
λ	tip speed ratio
P_r	rated power
δ_ω	percentage generator speed factor
φ	vector of coefficients of the polynomial for a surrogate model

1530 *Code and data availability.* Codes and data were created for each steps of the published method. However, some of the tools used are very specific to an in-house workflow and are only partially documented. Thus, there is no single self-contained program of which sharing would provide value for others. The dataset of load simulations will be shared publicly with the final revised paper. For inquiries about data or code, please reach out to the authors.

Author contributions. NR and TM developed the concept for the study and the research methods. NR developed the code and produced the results under supervision and with valuable input from TM. TM was responsible for project administration and funding acquisition. NR wrote the draft version of the paper. RH reviewed the draft version and gave valuable feedback on the draft, the concept and the results. TM and NR reviewed and edited the draft version.

Competing interests. The authors declare that they have no conflict of interest.

1540 *Acknowledgements.* The research was carried out by Fraunhofer IWES under the framework of two research projects funded by the Bundesministerium für Bildung und Forschung (BMBF): *H2-DIGITAL* (grant no. 03SF0635) and *Verbundvorhaben H2Mare_VB0: OffgridWind* (grant no. 03HY300E). Additionally, parts of the work were conducted within the project *DigiWind* in cooperation with TU Wien. TU Wien was funded by VGB Powertech e.V. in *DigiWind*.

References

- Andersson, L. E., Anaya-Lara, O., Tande, J. O., Merz, K. O., and Imsland, L.: Wind farm control – Part I: A review on control system concepts and structures, *IET Renewable Power Generation*, 37, 1703, <https://doi.org/10.1049/rpg2.12160>, 2021.
- 1545 Astrain Juangarcia, D., Eguinoa, I., and Knudsen, T.: Derating a single wind farm turbine for reducing its wake and fatigue, *Journal of Physics: Conference Series*, 1037, 032 039, <https://doi.org/10.1088/1742-6596/1037/3/032039>, 2018.
- Bastankhah, M. and Porté-Agel, F.: Experimental and theoretical study of wind turbine wakes in yawed conditions, *Journal of Fluid Mechanics*, 806, 506–541, <https://doi.org/10.1017/jfm.2016.595>, 2016.
- 1550 Bech, J. I., Hasager, C. B., and Bak, C.: Extending the life of wind turbine blade leading edges by reducing the tip speed during extreme precipitation events, *Wind Energy Science*, 3, 729–748, <https://doi.org/10.5194/wes-3-729-2018>, 2018.
- Beganovic, N. and Söffker, D.: Structural health management utilization for lifetime prognosis and advanced control strategy deployment of wind turbines: An overview and outlook concerning actual methods, tools, and obtained results, *Renewable and Sustainable Energy Reviews*, 64, 68–83, <https://doi.org/10.1016/j.rser.2016.05.083>, 2016.
- 1555 Biscani, F. and Izzo, D.: pygmo, <https://esa.github.io/pygmo2/index.html>, 2020a.
- Biscani, F. and Izzo, D.: A parallel global multiobjective framework for optimization: pagmo, *Journal of Open Source Software*, 5, 2338, <https://doi.org/10.21105/joss.02338>, 2020b.
- Bossanyi, E.: Combining induction control and wake steering for wind farm energy and fatigue loads optimisation, *Journal of Physics: Conference Series*, 1037, 032 011, <https://doi.org/10.1088/1742-6596/1037/3/032011>, 2018.
- 1560 Bossanyi, E.: Surrogate model for fast simulation of turbine loads in wind farms, *Journal of Physics: Conference Series*, 2265, 042 038, <https://doi.org/10.1088/1742-6596/2265/4/042038>, 2022.
- Bossanyi, E. and Jorge, T.: Optimisation of wind plant sector management for energy and loads, in: 2016 European Control Conference (ECC), pp. 922–927, IEEE, Piscataway, NJ, <https://doi.org/10.1109/ECC.2016.7810407>, 2016.
- Burton, T., Jenkins, N., Sharpe, D., and Bossanyi, E.: *Wind Energy Handbook*, John Wiley & Sons, Hoboken, 2 edn., <http://site.ebrary.com/lib/alltitles/docDetail.action?docID=10657218>, 2011.
- 1565 BVG Associates: Wind farm costs – Guide to an offshore wind farm, <https://guidetoanoffshorewindfarm.com/wind-farm-costs>, 2019.
- Chiandussi, G., Codegone, M., Ferrero, S., and Varesio, F. E.: Comparison of multi-objective optimization methodologies for engineering applications, *Computers & Mathematics with Applications*, 63, 912–942, <https://doi.org/10.1016/j.camwa.2011.11.057>, 2012.
- Debusscher, C. M. J., Göçmen, T., and Andersen, S. J.: Probabilistic surrogates for flow control using combined control strategies, *Journal of Physics: Conference Series*, 2265, 032 110, <https://doi.org/10.1088/1742-6596/2265/3/032110>, 2022.
- 1570 Dimitrov, N.: Surrogate models for parameterized representation of wake-induced loads in wind farms, *Wind Energy*, 22, 1371–1389, <https://doi.org/10.1002/we.2362>, 2019.
- Dimitrov, N., Kelly, M. C., Vignaroli, A., and Berg, J.: From wind to loads: wind turbine site-specific load estimation with surrogate models trained on high-fidelity load databases, *Wind Energy Science*, 3, 767–790, <https://doi.org/10.5194/wes-3-767-2018>, 2018.
- 1575 DNV GL: Certification of lifetime extension of wind turbines, 2016.
- Do, M. H. and Söffker, D.: State-of-the-art in integrated prognostics and health management control for utility-scale wind turbines, *Renewable and Sustainable Energy Reviews*, 145, 111 102, <https://doi.org/10.1016/j.rser.2021.111102>, 2021.

- Eguinoa, I., Göçmen, T., Garcia-Rosa, P. B., Das, K., Petrović, V., Kölle, K., Manjock, A., Koivisto, M. J., and Smailes, M.: Wind farm flow control oriented to electricity markets and grid integration: Initial perspective analysis, *Advanced Control for Applications*, 3, 1580 <https://doi.org/10.1002/adc2.80>, 2021.
- Elorza, I., Calleja, C., and Pujana-Arrese, A.: On Wind Turbine Power Delta Control, *Energies*, 12, 2344, <https://doi.org/10.3390/en12122344>, 2019.
- Fleming, P. A., Aho, J., Buckspan, A., Ela, E., Zhang, Y., Gevorgian, V., Scholbrock, A., Pao, L., and Damiani, R.: Effects of power reserve control on wind turbine structural loading, *Wind Energy*, 19, 453–469, <https://doi.org/10.1002/we.1844>, 2016.
- 1585 Gasparis, G., Lio, W. H., and Meng, F.: Surrogate Models for Wind Turbine Electrical Power and Fatigue Loads in Wind Farm, *Energies*, 13, 6360, <https://doi.org/10.3390/en13236360>, 2020.
- Harrison, M., Bossanyi, E., Ruisi, R., and Skeen, N.: An initial study into the potential of wind farm control to reduce fatigue loads and extend asset life, *Journal of Physics: Conference Series*, 1618, 022 007, <https://doi.org/10.1088/1742-6596/1618/2/022007>, 2020.
- Hersbach, H., Bell, B., Berrisford, P., Biavati, G., Horányi, A., Muñoz Sabater, J., Nicolas, J., Peubey, C., Radu, R., Rozum, I., 1590 Schepers, D., Simmons, A., Soci, C., Dee, D., and Thépaut, J.-N.: ERA5 hourly data on single levels from 1959 to present, <https://doi.org/10.24381/cds.adbb2d47>, 2018.
- Houck, D. R.: Review of wake management techniques for wind turbines, *Wind Energy*, 25, 195–220, <https://doi.org/10.1002/we.2668>, 2022.
- Hübler, C. and Rolfes, R.: Analysis of the influence of climate change on the fatigue lifetime of offshore wind turbines using imprecise probabilities, *Wind Energy*, 24, 275–289, <https://doi.org/10.1002/we.2572>, 2021.
- 1595 Hübler, C. J.: Efficient probabilistic analysis of offshore wind turbines based on time-domain simulations, Dissertation, Gottfried Wilhelm Leibniz Universität, Hannover, 2019.
- IEC: Wind Turbines - Part 1: Design Requirements, 2019.
- Jonkman, B. J.: TurbSim User's Guide: Version 1.50, NREL, 2009.
- Kanev, S., Bot, E., and Giles, J.: Wind Farm Loads under Wake Redirection Control, *Energies*, 13, 4088, <https://doi.org/10.3390/en13164088>, 1600 2020.
- Kanev, S. K., Savenije, F. J., and Engels, W. P.: Active wake control: An approach to optimize the lifetime operation of wind farms, *Wind Energy*, 21, 488–501, <https://doi.org/10.1002/we.2173>, 2018.
- Kölle, K., Göçmen, T., Eguinoa, I., Alcayaga Román, L. A., Aparicio-Sanchez, M., Feng, J., Meyers, J., Pettas, V., and Sood, I.: FarmConnors market showcase results: wind farm flow control considering electricity prices, *Wind Energy Science*, 7, 2181–2200, 1605 <https://doi.org/10.5194/wes-7-2181-2022>, 2022a.
- Kölle, K., Göçmen, T., Garcia-Rosa, P. B., Petrović, V., Eguinoa, I., Vrana, T. K., Long, Q., Pettas, V., Anand, A., Barlas, T. K., Cutululis, N., Manjock, A., Tande, J. O., Ruisi, R., and Bossanyi, E.: Towards integrated wind farm control: interfacing farm flow and power plant controls, *Advanced Control for Applications*, <https://doi.org/10.1002/adc2.105>, 2022b.
- Leimeister, M. and Thomas, P.: The OneWind Modelica Library for Floating Offshore Wind Turbine Simulations with Flexible Structures, 1610 in: *Proceedings of the 12th International Modelica Conference*, edited by Kofránek, J. and Casella, F., pp. 633–642, Modelica Association and Linköping University Electronic Press, Linköping, <https://doi.org/10.3384/ecp17132633>, 2017.
- Liao, D., Zhu, S.-P., Correia, J. A., de Jesus, A. M., Veljkovic, M., and Berto, F.: Fatigue reliability of wind turbines: historical perspectives, recent developments and future prospects, *Renewable Energy*, 200, 724–742, <https://doi.org/10.1016/j.renene.2022.09.093>, 2022.
- Lio, W. H., Mirzaei, M., and Larsen, G. C.: On wind turbine down-regulation control strategies and rotor speed set-point, *Journal of Physics: Conference Series*, 1037, 032 040, <https://doi.org/10.1088/1742-6596/1037/3/032040>, 2018. 1615

- Loepelmann, P. and Fischer, B.: Lifetime extension and opex reduction by adapting the operational strategy of wind farms, *Journal of Physics: Conference Series*, 2257, 012 014, <https://doi.org/10.1088/1742-6596/2257/1/012014>, 2022.
- Loew, S., Obradovic, D., and Bottasso, C. L.: Model predictive control of wind turbine fatigue via online rainflow-counting on stress history and prediction, *Journal of Physics: Conference Series*, 1618, 022 041, <https://doi.org/10.1088/1742-6596/1618/2/022041>, 2020.
- 1620 Lorenzo, C. F. and Merrill, W. C.: Life Extending Control - A Concept Paper, in: *American Control Conference*, 1991, pp. 1081–1095, IEEE, Piscataway, <https://doi.org/10.23919/ACC.1991.4791545>, 1991.
- Loth, E., Qin, C., Simpson, J. G., and Dykes, K.: Why we must move beyond LCOE for renewable energy design, *Advances in Applied Energy*, 8, 100 112, <https://doi.org/10.1016/j.adapen.2022.100112>, 2022.
- Manwell, J. F., McGowan, J. G., and Rogers, A. L.: *Wind energy explained: Theory, design and application*, Wiley, Chichester, 2. ed., repr. with cor edn., 2011.
- 1625 Mendez Reyes, H., Kanev, S., Doekemeijer, B., and van Wingerden, J.-W.: Validation of a lookup-table approach to modeling turbine fatigue loads in wind farms under active wake control, *Wind Energy Science*, 4, 549–561, <https://doi.org/10.5194/wes-4-549-2019>, 2019.
- Meng, F., Hou Lio, A. W., and Liew, J.: The effect of minimum thrust coefficient control strategy on power output and loads of a wind farm, *Journal of Physics: Conference Series*, 1452, 012 009, <https://doi.org/10.1088/1742-6596/1452/1/012009>, 2020.
- 1630 Meyer, T.: Optimization-based reliability control of mechatronic systems, Ph.D. Thesis, Universität Paderborn, <https://doi.org/10.17619/UNIPB/1-3>, 2016.
- Meyer, T., Fischer, K., Wenske, J., and Reuter, A.: Closed-loop supervisory control for defined component reliability levels and optimized power generation, in: *Windeurope Conference and Exhibition Proceedings*, http://publica.fraunhofer.de/eprints/urn_nbn_de_0011-n-5620801.pdf, 2017.
- 1635 Meyers, J., Bottasso, C., Dykes, K., Fleming, P., Gebraad, P., Giebel, G., Göçmen, T., and van Wingerden, J.-W.: Wind farm flow control: prospects and challenges, *Wind Energy Science*, 7, 2271–2306, <https://doi.org/10.5194/wes-7-2271-2022>, 2022.
- Miner, M. A.: Cumulative Damage in Fatigue, *Journal of Applied Mechanics*, 12, A159–A164, <https://doi.org/10.1115/1.4009458>, 1945.
- Mozafari, S., Dykes, K., Rinker, J. M., and Veers, P.: Effects of finite sampling on fatigue damage estimation of wind turbine components: A statistical study, *Wind Engineering*, p. 0309524X2311638, <https://doi.org/10.1177/0309524X231163825>, 2023.
- 1640 Nash, R., Nouri, R., and Vassel-Be-Hagh, A.: Wind turbine wake control strategies: A review and concept proposal, *Energy Conversion and Management*, 245, 114 581, <https://doi.org/10.1016/j.enconman.2021.114581>, 2021.
- Nielsen, J. S., Miller-Branovacki, L., and Carriveau, R.: Probabilistic and Risk-Informed Life Extension Assessment of Wind Turbine Structural Components, *Energies*, 14, 821, <https://doi.org/10.3390/en14040821>, 2021.
- Njiri, J. G. and Söffker, D.: State-of-the-art in wind turbine control: Trends and challenges, *Renewable and Sustainable Energy Reviews*, 60, 377–393, <https://doi.org/10.1016/j.rser.2016.01.110>, 2016.
- 1645 Njiri, J. G., Beganovic, N., Do, M. H., and Söffker, D.: Consideration of lifetime and fatigue load in wind turbine control, *Renewable Energy*, 131, 818–828, <https://doi.org/10.1016/j.renene.2018.07.109>, 2019.
- Pettas, V. and Cheng, P. W.: Down-regulation and individual blade control as lifetime extension enablers, *Journal of Physics: Conference Series*, 1102, 012 026, <https://doi.org/10.1088/1742-6596/1102/1/012026>, 2018.
- 1650 Pettas, V., Salari, M., Schlipf, D., and Cheng, P. W.: Investigation on the potential of individual blade control for lifetime extension, *Journal of Physics: Conference Series*, 1037, 032 006, <https://doi.org/10.1088/1742-6596/1037/3/032006>, 2018.
- Popko, W., Thomas, P., Sevinc, A., Rosemeier, M., Bätge, M., Braun, R., Meng, F., Horte, D., and Balzani, C.: IWES Wind Turbine IWT-7.5-164. Rev 4, Fraunhofer IWES, Bremerhaven, <https://doi.org/10.24406/IWES-N-518562>, 2018.

- Pryor, S. C., Shepherd, T. J., and Barthelmie, R. J.: Interannual variability of wind climates and wind turbine annual energy production, *Wind Energy Science*, 3, 651–665, <https://doi.org/10.5194/wes-3-651-2018>, 2018.
- 1655 Rakowsky, K. U.: An introduction to Reliability-Adaptive Systems, in: *Advances in Safety and Reliability*, edited by Kolowrocki, K., pp. 1633–1636, 2005.
- Rakowsky, U. K.: Modelling Reliability-Adaptive multi-system operation, *International Journal of Automation and Computing*, 3, 192–198, <https://doi.org/10.1007/s11633-006-0192-8>, 2006.
- 1660 Requate, N. and Meyer, T.: Active Control of the Reliability of Wind Turbines, *IFAC-PapersOnLine*, 53, 12 789–12 796, <https://doi.org/10.1016/j.ifacol.2020.12.1941>, 2020.
- Requate, N., Wiens, M., and Meyer, T.: A Structured Wind Turbine Controller Evaluation Process Embedded into the V-Model for System Development, *Journal of Physics: Conference Series*, 1618, 022 045, <https://doi.org/10.1088/1742-6596/1618/2/022045>, 2020.
- Santos, R. A.: Damage mitigating control for wind turbines, Ph.D. Thesis, The University of Colorado, Colorado, 2006.
- 1665 Santos, R. A.: Control system for wind turbine, 2008.
- Schmidt, J.: FOXES, <https://fraunhoferiwes.github.io/foxes.docs/index.html>, 2022.
- Schmidt, J., Requate, N., and Vollmer, L.: Wind Farm Yield and Lifetime Optimization by Smart Steering of Wakes, *Journal of Physics: Conference Series*, 1934, 012 020, <https://doi.org/10.1088/1742-6596/1934/1/012020>, 2021.
- Singh, D., Dwight, R. P., Laugesen, K., Beaudet, L., and Viré, A.: Probabilistic surrogate modeling of offshore wind-turbine loads with chained Gaussian processes, *Journal of Physics: Conference Series*, 2265, 032 070, <https://doi.org/10.1088/1742-6596/2265/3/032070>, 2022.
- 1670 Slot, R. M., Sørensen, J. D., Sudret, B., Svenningsen, L., and Thøgersen, M. L.: Surrogate model uncertainty in wind turbine reliability assessment, *Renewable Energy*, 151, 1150–1162, <https://doi.org/10.1016/j.renene.2019.11.101>, 2020.
- Söffker, D. and Rakowsky, U. K.: Perspectives of monitoring and control of vibrating structures by combining new methods of fault detection with new approaches of reliability engineering, *A Critical Link: Diagnosis to Prognosis*, pp. 671–682, 1997.
- 1675 Sutherland, H. J.: On the Fatigue Analysis of Wind Turbines, Sandia National Labs., Albuquerque, NM (US), Sandia National Laboratories, Albuquerque, New Mexico, <https://doi.org/10.2172/9460>, 1999.
- Thomas, P.: MoWiT, www.mowit.info, 2022.
- Thomas, P., Gu, X., Samlaus, R., Hillmann, C., and Wihlfahrt, U.: The OneWind Modelica Library for Wind Turbine Simulation with Flexible Structure - Modal Reduction Method in Modelica, in: *Proceedings of the 10th International Modelica Conference*, Linköping Electronic Conference Proceedings, pp. 939–948, Linköping University Electronic Press, <https://doi.org/10.3384/ecp14096939>, 2014.
- 1680 van der Hoek, D., Kanev, S., and Engels, W.: Comparison of Down-Regulation Strategies for Wind Farm Control and their Effects on Fatigue Loads, in: *2018 Annual American Control Conference (ACC)*, pp. 3116–3121, IEEE, <https://doi.org/10.23919/ACC.2018.8431162>, 2018.
- Waechter, A. and Laird, C.: Ipopt, <https://coin-or.github.io/Ipopt/index.html>, 2022.
- 1685 Wiens, M.: Turbine operation: Control systems keep everything running smoothly, <https://websites.fraunhofer.de/IWES-Blog/en/turbine-operation-control-systems-keep-everything-running-smoothly/marcus-wiens>, 2021.
- Zhu, J., Ma, K., Soltani, M., Hajizadeh, A., and Chen, Z.: Comparison of loads for wind turbine down-regulation strategies, in: *2017 Asian Control Conference Gold Coast*, Australia, pp. 2784–2789, IEEE, Piscataway, NJ, <https://doi.org/10.1109/ASCC.2017.8287618>, 2017.